

Pharmacological Evaluation of *Imperata Cylindrica* Crude Extract as Anti-Angiogenic Potential: Network Pharmacology, Molecular Docking Prediction with ADMET Analysis and CAM Assay Visualization

Sheemaiah Kyle L. Hasim., Mary Chris M. Castillo., Riza Jane T. Andig., Julio Raymundo M. Pasagui.,
Judie L. Velasco

STEM Department, Carlos P. Garcia Senior High School, Davao City, Philippines

DOI: <https://doi.org/10.51244/IJRSI.2026.13020055>

Received: 13 February 2026; Accepted: 18 February 2026; Published: 28 February 2026

ABSTRACT

This study investigated the anti-angiogenic potential of *Imperata cylindrica* (cogon grass) leaf extract through an integrated network pharmacology-guided in silico approach coupled with in vivo validation, focusing on the multi-target behavior of its bioactive compounds. Given the central role of angiogenesis in tumor growth and metastasis, identifying plant-derived compounds capable of modulating angiogenic pathways remains a strategic priority in cancer research.

Network pharmacology analysis identified ten major bioactive compounds with high relevance to angiogenesis-associated pathways. Salicin and Jaceidin emerged as the most influential compounds, exhibiting the highest network degree values (degree = 34), followed by Caffeic acid (degree = 33), Tricin (27), Ferulic acid (26), Ethyl p-Hydroxybenzoate (24), Flavone and N-Acetyl-p-aminophenol (23), p-Vinylguaiacol (18), and 2-Methoxysterone (17). KEGG pathway enrichment further confirmed that these compounds were strongly associated with angiogenesis-related signaling cascades, while non-connected pathways were excluded to ensure biological relevance.

Subsequent molecular docking analyses demonstrated stable and favorable binding interactions between the top-ranked compounds and key angiogenic targets, particularly vascular endothelial growth factor receptor-2 (VEGFR-2) and protein kinase B (AKT1), supporting their predicted role as multi-target angiogenesis inhibitors. ADMET profiling further suggested acceptable pharmacokinetic and safety properties for the leading compounds.

Biological validation using the chick embryo chorioallantoic membrane (CAM) assay revealed a clear dose-dependent inhibition of neovascularization following treatment with *I. cylindrica* leaf extract. The highest tested concentration (30 µg/mL) produced the most pronounced reduction in blood vessel density and branching, with no observable embryotoxic effects.

Collectively, these findings demonstrate that *I. cylindrica* leaf extract exerts anti-angiogenic activity through multi-compound, multi-target mechanisms, with Salicin, Jaceidin, and Caffeic acid acting as central network regulators. The study supports the potential of *I. cylindrica* as a source of natural anti-angiogenic agents and recommends further compound isolation, mechanistic validation, and advanced in vivo studies to establish therapeutic applicability in cancer treatment.

Keywords: *Imperata cylindrica*, angiogenesis, bioactive compounds

INTRODUCTION

Angiogenesis, a development of new blood vessels from pre-existing ones, is an essential component of cancer development and progression (Al-Ostoot et al., 2021). Without a sufficient blood supply, tumors cannot

metastasize to other parts of the body or develop larger than a microscopic size (Costa, 2025). Tumor growth and metastasis depend on angiogenesis, which creates new blood vessels enabling tumors to absorb nutrients and oxygen (Lugano et al., 2020). Without vascular support, tumors stop growing or become necrotic. This process requires both activation of angiogenic factors and suppression of inhibitors to successfully form new vessels (Nishida et al., 2022). Uncontrolled angiogenesis may lead to several angiogenic disorders, including vascular insufficiency (myocardial or critical limb ischemia) and vascular overgrowth (hemangiomas, vascularized tumors, and retinopathies) (Yoo & Kwon, 2013). There is accumulating evidence that many diseases are angiogenesis dependent. Pathological angiogenesis is a hallmark of many cancers, diabetic retinopathy, autoimmune diseases, rheumatoid arthritis, atherosclerosis, cerebral ischemia, cardiovascular diseases, and delayed wound healing (Fallah et al. 2019). Due to its critical function in tumor survival and dissemination, angiogenesis is now viewed as a target of central importance in approaches to cancer therapy. As this serious problem continues to grow, it becomes more urgent to have an effective alternative for suppressing angiogenesis.

Angiogenesis plays a critical role in the growth of cancer because solid tumors need a blood supply if they are to grow beyond a few millimeters in size (National Cancer Institute 2018). Breast cancer cells, like all body tissues, need constant nourishment and oxygen supply through the vascular network of capillaries in the system (Gill & Vishwanatha 2016). It is estimated that about 270,000 new cases of invasive breast cancer are projected to be diagnosed in women in the U.S. in 2018 (American Cancer Society 2024). Diabetic retinopathy, a DM microvascular complication, is the leading cause of blindness. Angiogenic factors such as vascular endothelial growth factor (VEGF) are involved in the pathogenesis of diabetic retinopathy (Valliati et al. 2011). Ninety-three million people are globally affected by diabetic retinopathy (Shukla & Tripathy 2023). Angiogenesis, the development of new capillaries, is involved in leukocyte ingress into the synovium during the development and progression of rheumatoid arthritis (Szekanecz & Koch 2009). In 2019, 18 million people worldwide were living with rheumatoid arthritis (World Health Organization 2023). Intraplaque angiogenesis, a critical mechanism in the pathological progression of atherosclerosis (AS), exhibits a paradoxical role by providing nutrients and repair support for plaques while simultaneously contributing to plaque instability and rupture (Yan et al. 2025). In America, about half of people aged 45 to 84 have atherosclerosis but aren't aware of it, according to the U.S. National Institutes of Health.

In the Philippines, cancer incidence and mortality are significant and growing concerns. According to the WHO-GLOBOCAN 2022 data, there were 188,976 new cancer cases in the country (all cancer types, both sexes) in 2022. In an earlier national cancer profile (2018), it was estimated there were 141,021 total cancer cases and 86,337 deaths in that year. The disease burden is exacerbated by shortages of oncology specialists—there are about 348 medical oncologists, 164 surgical oncologists, and 99 radiation oncologists nationwide for a population nearing 110 million (Garcia et al., 2022). Diabetic retinopathy (DR) is a major complication among people with diabetes in the Philippines. In 2021, it was estimated that 4.3 million Filipinos had been diagnosed with diabetes (and an additional 2.8 million were undiagnosed). A telemedicine screening study of Filipino type-2 diabetic patients found that among 195 participants (387 eyes examined), 25.26% had some degree of diabetic retinopathy (3.16% mild, 15.79% moderate, 3.68% severe, 3.68% proliferative). Separately, a media release estimated that about 200,000 Filipinos suffer from diabetic retinopathy or maculopathy (Lopez et al., 2022). Cardiovascular diseases (CVDs) remain the leading cause of death in the Philippines. In 2021, there were 225,939 deaths attributed to CVDs nationwide. In 2022, ischemic heart diseases alone were responsible for 114,557 deaths, equivalent to 18.4% of all recorded deaths. More recently, from January to November 2024, 96,049 deaths (19.3% of total) were attributed to ischemic heart disease (Santos et al., 2022).

In 2020, neoplasms (cancer) accounted for 3,164 deaths in the Davao Region, representing 10.1% of the total 31,270 registered deaths. Among the provinces and cities, the City of Davao recorded the highest number of deaths overall (10,917), which implies a substantial share of cancer mortality likely originates there (Philippine Statistic Authority, 2022). Gender disaggregation shows more male deaths (18,468) than female (12,802) for all causes in the Davao Region, suggesting the male burden of cancer deaths may be higher, although specific cancer rates by sex were not broken down. Previous reports indicate that a health-screening initiative in Davao referred 105 diabetic patients over two Saturdays for retinopathy testing under a program offered free of charge and without patient-number limits, though no disaggregation by retinopathy severity was reported (Malabanan-

Cabebe et al., 2024). In a concurrent analysis involving 157 patients, 46% were female, 44% resided in the Davao region, and 69% manifested unilateral disease. Meanwhile, data from the Southern Philippines Medical Center–Adult Cancer Center (SPMC-ACC) reveal that cancer cases escalated to 14,909 in 2022 (compared to 10,439 in 2021), with 746 inpatients, 7,375 outpatients, 2,673 via teleconsult, 914 new diagnoses, and 3,201 patients receiving infusion therapy. Cardiovascular diseases, particularly diseases of the heart, remain a leading cause of mortality in the Davao Region, with DOH–Davao reporting 3,216 heart disease deaths in 2022 and 2,528 in 2023. In a clinical study in Davao City examining heart failure patients, higher NT-proBNP levels correlated with lower left ventricular ejection fraction and were predictive of in-hospital mortality (Patumbon, 2023). The 2020 PSA special release shows cerebrovascular diseases (e.g., stroke) accounted for 3,948 deaths (12.6% of total) in the region, making them a significant component of cardiovascular mortality (Philippine Statistic Authority, 2022).

Although angiogenesis plays a vital role in the progression of cancer and other diseases such as diabetic retinopathy, rheumatoid arthritis, and atherosclerosis, current treatment options remain limited by high cost, side effects, and reduced long-term effectiveness. This highlights the need for safer and more affordable natural alternatives that can suppress abnormal blood vessel formation. *I. cylindrica*, a medicinal plant known for its antioxidant, anti-inflammatory, and anticancer properties, remains underexplored for its anti-angiogenic potential. In the Philippines, where the prevalence of cancer, cardiovascular diseases, and diabetes complications continues to rise—particularly in regions like Davao—there is a growing need to discover local plant-based therapies that may help address these conditions. Thus, this study aims to fill this gap by evaluating the anti-angiogenic potential of *I. cylindrica* crude extract through network pharmacology, molecular docking prediction, and CAM assay visualization.

Statement of the Problem

This study aligned with SDG 3: Good Health and Well-being, as it investigated the anti-angiogenic effects of *I. cylindrica* crude extract. By exploring plant extracts for their potential therapeutic benefits, this research supported SDG 3's goal of improving health and well-being by offering new, sustainable, and accessible treatment options. The study sought to answer the following:

1. What is the concentration of *Imperata cylindrica* crude extract required to produce anti-angiogenic activity in the CAM assay?
2. What is the observable anti-angiogenic activity of *Imperata cylindrica* crude extract in the CAM assay in terms of:
 - 2.1. Vascular Junctions
 - 2.2. End-Point Voxels
 - 2.3. Maximum Branch Length
3. How do the bioactive compounds in *Imperata cylindrica* crude extract interact with molecular targets to modulate angiogenesis, in terms of:
 - 3.1. Kyoto Encyclopedia of Genes and Genomes (KEGG) Pathways
 - 3.2. Gene Ontology Biological Process (BP)
 - 3.3. Gene Ontology Cellular Component (CC)
 - 3.4. Gene Ontology Molecular Function (MF)
4. What is the predicted anti-angiogenic interaction between the phytochemicals in *Imperata cylindrica* crude extract and VEGFR-2, based on molecular docking analysis?

5. Is there a significant difference in anti-angiogenic effect between *Imperata cylindrica* crude extract and the negative control group?

Research Hypothesis

H₀: There is no significant anti-angiogenic activity exhibited by *Imperata cylindrica* crude extract.

Significance of the Study

This study aligns closely with SDG 3: Good Health and Well-being, which aims to ensure healthy lives and promote well-being for all ages. By investigating the anti-angiogenic effects of *I. cylindrica* crude extract, the research explores natural, plant-based compounds with potential therapeutic benefits. These compounds may offer new approaches to treating diseases driven by abnormal blood vessel formation, such as cancer and diabetic complications. This aligns with SDG 3's emphasis on advancing research and development of safe, effective, and affordable medicines.

Department of Health (DOH), Philippines. The DOH may consider this research in the context of the use of *I. cylindrica*, which could support health programs targeting conditions involving abnormal blood vessel formation, thereby improving patient outcomes using locally available resources.

Department of Science and Technology (DOST), Philippines. By supporting studies like this, the DOST advances its mission to foster scientific research and innovation. The study promotes the sustainable use of native plant species for potential medical applications, aligning with national priorities in health and biotechnology.

City health governments. can utilize the findings of this study to promote community-based health initiatives that encourage the use of native medicinal plants. This supports the development of affordable, accessible treatment options at the local level, fostering healthier communities through sustainable healthcare practices.

Local residents and communities. This study highlights the potential of native plants like *I. cylindrica* as accessible, sustainable health resources. It encourages awareness and acceptance of natural remedies, fostering community engagement in health promotion and disease prevention.

Future Researchers. This study provides a valuable foundation for future scientific inquiry. It encourages further exploration into the medicinal properties of native plants, particularly in relation to angiogenesis, and serves as a reference point for students and professionals interested in natural product research and sustainable health solutions.

Scope and Delimitation

This study investigated the anti-angiogenic potential of *I. cylindrica* crude extract, focusing on its effects in inhibiting blood vessel formation. The research employed molecular docking to examine interactions between the extract's top phytochemical and VEGFR-2, network pharmacology to predict compound-target interactions and pathways, and the Chorioallantoic Membrane (CAM) assay to observe vascular changes in response to different extract concentrations. Comparative analyses were conducted using negative and positive controls to evaluate the extract's efficacy. The study aimed to provide insights into the therapeutic potential of *I. cylindrica* as a natural anti-angiogenic agent.

The study was limited to in vitro and in silico analyses, specifically molecular docking, network pharmacology predictions, and CAM assay experiments, without involving in vivo mammalian models. Due to the lack of advanced equipment locally, no phytochemical analysis was performed to characterize the exact composition of the *I. cylindrica* crude extract used. Therefore, variations in phytochemical content depending on extraction methods and plant sources may have affected the consistency of results. Additionally, computational predictions may not have fully represented complex biological interactions. The focus was exclusively on anti-angiogenic effects, excluding other pharmacological activities or clinical evaluations of the extract. The total number of fertilized eggs for the experiment was limited due to constraints in the supply chain, specifically, the low production capacity of the local vendor's chicken flock. The study's results are critically limited by pseudo-

replication, as the biological sample size was restricted to N=1 egg per treatment group, thereby preventing valid statistical generalization.

Definition of Terms

The following terms were operationally defined:

Angiogenesis, also known as anti-angiogenic therapies, refers to a type of cancer treatment that aims to starve tumors by preventing the development of new blood vessels.

Embryonic Development Day refers to the initial stages of an organism's development, from fertilization to the formation of a fetus. In humans, this period typically lasts from the third to the eighth week of pregnancy.

Imperata Cylindrica commonly known as cogon grass, is a resilient perennial grass species that can thrive in a variety of soil conditions, including acidic and clay soils, and can survive drought, high salinity, and shade. It has significant ecological applications, such as absorbing lead from contaminated soils and serving as a source for catalysts in the conversion of waste plastic to fuel oil.

3B8R. The entry code in the Protein Data Bank for the crystal structure of the Vascular Endothelial Growth Factor Receptor 2 Kinase Domain complexed with a Naphthamide Inhibitor.

4ASD. The entry code in the Protein Data Bank for the crystal structure of the Vascular Endothelial Growth Factor Receptor 2 Kinase Domain complexed with the FDA-approved drug Sorafenib (also known as BAY 43-9006).

METHODOLOGY

This section presented the methodology of the study, which was conducted in four (4) phases: Phase I – Compound Preparation; Phase II – In Vivo Assay (Chorioallantoic Membrane Assay); Phase III – Network Pharmacology; and Phase IV – Molecular Docking. All tests and experimental procedures were carried out at Carlos P. Garcia Senior High School.

Research Design

An experimental-quantitative research design was used in this study to collect related data and information. According to Grand Canyon University (2025), experimental quantitative research design utilized the scientific approach. It established procedures that allowed the researcher to test a hypothesis and to systematically and scientifically study causal relationships among variables. An appropriate experimental design acted as a roadmap for the research techniques, giving readers a better understanding of the data collection process and, as a result, allowed an exact description of the findings.

This study utilized an experimental-quantitative research design to evaluate the anti-angiogenic potential of crude extract from *I. cylindrica*. The research employed in silico molecular docking to predict the interaction of the highest concentration of phytochemicals in *I. cylindrica* crude extract with angiogenesis receptor proteins and network pharmacology to identify related biological targets and pathways involved in angiogenesis. Additionally, an in vitro chick embryo chorioallantoic membrane (CAM) assay was used to measure its inhibitory effect on angiogenesis. These approaches generated quantifiable data that supported a systematic analysis of *I. cylindrica* crude extract anti-angiogenic activity.

Phytochemicals of *Imperata Cylindrica*

Imperata cylindrica is a medicinal plant native to southwestern Asia and the tropical and subtropical zones. To date, 72 chemical constituents have been isolated and identified from *I. cylindrica*. Among the constituents isolated from *I. cylindrica*, saponins, glycosides, flavonoids, coumarins, and phenols are the primary types (Jung & Shin 2021).

Table 1. Phytochemicals of *Imperata cylindrica*

No.	Name	CAS	Formula
Saponins			
1	Arundoin	4555-56-0	C ₃₁ H ₅₂ O
2	Cylindrin	17904-55-1	C ₃₁ H ₅₂ O
3	26-Norolean-9(11)-ene, 3-methoxy-13-methyl-, (3β)-	2392-92-9	C ₃₁ H ₅₂ O
4	(8α)-Arborinol methyl ether	27570-19-0	C ₃₁ H ₅₂ O
5	β-Sitosterol	83-46-5	C ₂₉ H ₅₀ O
6	Daucosterol	474-58-8	C ₃₅ H ₆₀ O ₆
7	α-Amyrin	638-95-9	C ₃₀ H ₅₀ O
8	3-O-β-D-glucopyranosyl-6'-tetradecanoate	120000-27-3	C ₄₉ H ₈₆ O ₇
9	Friedelin	559-74-0	C ₃₀ H ₅₀ O
10	Alnusenone	508-09-8	C ₃₀ H ₄₈ O
11	Simiarenol	1615-94-7	C ₃₀ H ₅₀ O
12	Fernenol	4966-00-1	C ₃₀ H ₅₀ O
13	2-Methoxyestrone	362-08-3	C ₁₉ H ₂₄ O ₃
14	14-epiarbor-7-en-3β-ol	-	C ₃₀ H ₅₀ O
15	14-epiarbor-7-en-3β-yl formate	-	C ₃₁ H ₅₀ O ₂
16	14-epiarbor-7-en- 3-one	-	C ₃₀ H ₄₈ O
Flavonoids			
17	Tricin	520-32-1	C ₁₇ H ₁₄ O ₇
18	Caryatin	1486-66-4	C ₁₇ H ₁₄ O ₇
19	Jaceidin	10173-01-0	C ₁₈ H ₁₆ O ₈
20	4 <i>H</i> -1-Benzopyran-4-one, 7-hydroxy-2-(4-hydroxy-3-methoxyphenyl)-3,5,6-trimethoxy-	58130-92-0	C ₁₉ H ₁₈ O ₈
21	5-Methoxyflavone	42079-78-7	C ₁₆ H ₁₂ O ₃
22	5-Hydroxyflavone	491-78-1	C ₁₅ H ₁₀ O ₃
23	Flavone	525-82-6	C ₁₅ H ₁₀ O ₂
24	2-(4-Hydroxyphenyl)-5-methoxy-4 <i>H</i> -1-benzopyran-4-one	106848-87-7	C ₁₆ H ₁₂ O ₄

25	4 <i>H</i> -1-Benzopyran-4-one, 6-(β -D-glucopyranosyloxy)-2-(4-methoxyphenyl)-	1588495-01-5	C ₂₂ H ₂₂ O ₉
26	5,7-Dihydroxy-8-methoxyflavone	632-85-9	C ₁₆ H ₁₂ O ₅
27	6-Hydroxy-5-methoxy-2-phenyl-4 <i>H</i> -1-benzopyran-4-one	118021-60-6	C ₁₆ H ₁₂ O ₄
28	5-hydroxy-2-(2-phenylethyl) chromone	877673-99-9	C ₁₇ H ₁₄ O ₃
29	Flindersiachromone	61828-53-3	C ₁₇ H ₁₄ O ₂
30	5-Hydroxy-2-[2-(2-hydroxyphenyl)ethyl]-4 <i>H</i> -1-benzopyran-4-one	357637-15-1	C ₁₇ H ₁₄ O ₄
31	5-Hydroxy-2-(2-phenylethenyl)-4 <i>H</i> -1-benzopyran-4-one	389136-26-9	C ₁₇ H ₁₂ O ₃
32	Flindersiachromone	61828-53-3	C ₁₇ H ₁₄ O ₂
33	4 <i>H</i> -1-Benzopyran-4-one, 5-hydroxy-2-(2-phenylethyl)-	877673-99-9	C ₁₇ H ₁₄ O ₃
34	8-Hydroxy-2-(2-phenylethyl)-4 <i>H</i> -1-benzopyran-4-one	1588494-99-8	C ₁₇ H ₁₄ O ₃
35	4 <i>H</i> -1-Benzopyran-4-one, 8-(β -D-glucopyranosyloxy)-2-(2-phenylethyl)	1588495-00-4	C ₂₃ H ₂₄ O ₈
36	Maritimin	3449-40-9	C ₁₁ H ₁₀ O ₄
Glycosides			
37	Salicin	138-52-3	C ₁₃ H ₁₈ O ₇
38	3,4-Dimethoxyphenyl 1- <i>O</i> - α -L-rhamnopyranosyl-(1 \rightarrow 6)- <i>O</i> - β -D-glucopyranoside	872885-48-8	C ₂₀ H ₃₀ O ₁₂
39	Seguinoside K	257888-26-9	C ₂₆ H ₃₂ O ₁₅
40	Gymnetinoside D	1588477-87-5	C ₂₇ H ₃₄ O ₁₅
41	Deacetylimpecyloside	1622990-04-8	C ₃₂ H ₃₈ O ₁₇
42	Impecyloside	1070967-17-7	C ₃₄ H ₄₀ O ₁₈
Phenols			
43	Graminone B	161407-73-4	C ₂₁ H ₂₂ O ₈
44	Graminone A	161407-72-3	C ₂₀ H ₂₀ O ₇
45	Cylindol A	159225-89-5	C ₁₆ H ₁₄ O ₇
46	Cylindol B	159225-90-8	C ₁₆ H ₁₄ O ₇
47	Imperanene	163634-08-0	C ₁₉ H ₂₂ O ₅
48	4-Hydroxy-cinnamic acid	57-10-3	C ₁₆ H ₃₂ O ₂

49	Isovanillin	621-59-0	C ₈ H ₈ O ₃
50	Ethyl p-hydroxybenzoate	120-47-8	C ₉ H ₁₀ O ₃
51	Vanillic acid	121-34-6	C ₈ H ₈ O ₄
52	p-Vinylguaiacol	7786-61-0	C ₉ H ₁₀ O ₂
53	Protocatechuic acid	99-50-3	C ₇ H ₆ O ₄
54	1-O-p-Coumaroylglycerol	63529-09-9	C ₁₂ H ₁₄ O ₅
55	4-Hydroxybenzaldehyde	123-08-0	C ₇ H ₆ O ₂
56	Impecylone	1622990-03-7	C ₁₄ H ₁₄ O ₄
57	Impecylenolide	1622990-05-9	C ₂₀ H ₂₀ O ₇
58	Caffeic acid	331-39-5	C ₉ H ₈ O ₄
59	Ferulic acid	1135-24-6	C ₁₀ H ₁₀ O ₄
60	N-Acetyl-p-aminophenol	103-90-2	C ₈ H ₉ NO ₂
Coumarins			
61	Siderin	53377-54-1	C ₁₂ H ₁₂ O ₄
62	7-O-Glucosyloxy-4-methoxy-5-methylcoumarin	41680-13-1	C ₁₇ H ₂₀ O ₉
63	7-Hydroxy-4-methoxy-5-methylcoumarin	41680-12-0	C ₁₁ H ₁₀ O ₄
Other Compounds			
64	Dimethyl 4,4'-dimethoxy-5,6,5',6'-dimethylenedioxybiphenyl-2,2'-dicarboxylate	73536-69-3	C ₂₀ H ₁₈ O ₁₀
65	Palmitic acid	57-10-3	C ₁₆ H ₃₂ O ₂
66	Cylindrene	158204-49-0	C ₁₅ H ₂₀ O ₂
67	5-Hydroxymethylfurfural	67-47-0	C ₆ H ₆ O ₃
68	Phytol	150-86-7	C ₂₀ H ₄₀ O
69	Tabanone	13215-88-8	C ₁₃ H ₁₈ O
70	3-(3,4,5-Trimethoxyphenoxy)-1,2-propanediol	68576-87-4	C ₁₂ H ₁₈ O ₆
71	3, 4-Dihydroxybutyric acid	1518-61-2	C ₄ H ₈ O ₄
72	L-Cysteine	52-90-4	C ₃ H ₇ NO ₂ S

Note. From "Imperata Cylindrica: A Review of Phytochemistry, Pharmacology, and Industrial Applications," by Y.-K. Jung and D. Shin, 2021, *Molecules*, 26(5), 1454. <https://doi.org/10.3390/molecules26051454>.

Reprinted under the terms of the Creative Commons Attribution (CC BY) license.

The concentrations of 10 $\mu\text{g/mL}$, 20 $\mu\text{g/mL}$, and 30 $\mu\text{g/mL}$ of *I. cylindrica* crude extract were selected based on literature precedent from CAM and anti-angiogenic plant extract studies showing effective activity at low doses. For example, Seo et al. (2013) screened 59 Korean medicinal plant extracts in a chick chorioallantoic membrane (CAM) assay at 10 $\mu\text{g/mL}$, demonstrating measurable inhibition of capillary growth. Similarly, Awasthi et al. (2020) reported significant anti-angiogenic effects of *Callistemon citrinus* flower extract in the CAM assay at concentrations ranging from 3.125 to 25 $\mu\text{g/egg}$, with the most notable inhibition observed between 12.5–25 $\mu\text{g/egg}$. Lee et al. (2015) also observed inhibition of vascular endothelial growth factor (VEGF)-induced angiogenesis using *Nelumbo nucifera* leaf extract at 10–100 $\mu\text{g/mL}$, further supporting the selection of low- $\mu\text{g/mL}$ concentrations for anti-angiogenic assays. Published cytotoxicity data for *I. cylindrica* report activity near 20 $\mu\text{g/mL}$ in cell assays (Kuetze et al., 2011), supporting 20 $\mu\text{g/mL}$ as a defensible upper bound for initial testing.

Guided by these studies and preliminary range-finding tests confirming embryo viability, 10 $\mu\text{g/mL}$, 20 $\mu\text{g/mL}$ and 30 $\mu\text{g/mL}$ were chosen as reference concentrations, and to evaluate potential dose-dependent characteristics of angiogenesis inhibition. Although direct CAM data on *I. cylindrica* are unavailable, the concentrations were guided by comparable plant extract studies employing the same biological assay and targeting similar mechanisms of angiogenesis inhibition. Thus, this range was selected to ensure methodological comparability, biological relevance, and safety within the embryo model.

Phase I – Compound Preparation

The entire process encompassed extraction, purification, and preparation of stock solution. Each phase involved specific steps such as maceration, rotary evaporation, and appropriate storage to ensure the stability and usability of the final crude extract.

Plant Collection

Imperata cylindrica (Cogon Grass), Poaceae family, was collected on September 14, 2025, by researchers in Purok-43, Victoria Christian Village, Barangay Ilang, Bunawan district, Davao city, Philippines.

Extraction

The leaves of *I. cylindrica* were collected and thoroughly washed with distilled water. The plant material was air-dried at room temperature for 7 days in the shade and ground into a fine powder. The powdered plant material was then soaked in 80% ethanol and subjected to maceration at room temperature for 5 days, with occasional stirring.

Purification

The purification of the plant extract was carried out using a rotary evaporator to remove the solvent and obtain a concentrated crude extract. This method worked by applying gentle heat and reduced pressure, allowing the solvent to evaporate efficiently at a lower temperature, which helped preserve the bioactive compounds present in the extract (Azwanida, 2015). The ethanolic extract of *I. cylindrica* was concentrated using a rotary evaporator set at 45°C under reduced pressure to efficiently remove the solvent without degrading heat-sensitive phytochemicals. This temperature range was commonly used for ethanol-based extractions to preserve the integrity of bioactive compounds and obtain a stable crude extract (Abubakar & Haque, 2020).

Storage

The crude extract of *I. cylindrica* obtained after rotary evaporation was stored to maintain its stability and prevent degradation of bioactive compounds. The extract was transferred into an amber glass container to protect it from light exposure and stored at 4°C until further experimental use. Proper storage at low temperature minimized oxidation, microbial growth, and chemical degradation, thereby preserving the phytochemical integrity of the extract (Azwanida, 2015). Refrigerated storage was a standard practice in natural product research to ensure that

plant extracts remained chemically stable and biologically active for extended periods (Abubakar & Haque, 2020).

Phase II – In Vivo Assay (Chorioallantoic Membrane Assay)

The CAM assay was utilized to evaluate the anti-angiogenic activity of *I. cylindrica* extract, as it provided a suitable in vivo model for observing blood vessel inhibition. The CAM angiogenesis assay was performed by implanting a filter paper disk containing the compound of interest on the chick embryo chorioallantoic membrane through a hole cut in the eggshell. The Institutional Animal Care and Use Committee (IACUC), an association of New England Medical Center and Tufts, as well as the National Institutes of Health, USA, mandated that a chick embryo that had not reached the 14th day of its gestation period would not experience pain and could therefore be used for experimentation without any ethical restrictions or prior protocol approval, simplifying the planning process.

Egg Preparation

Fresh, 14 fertilized chicken eggs were collected from a local vendor in Davao City and immediately incubated at 37°C with 60% relative humidity to initiate embryonic development. The eggs were placed with the narrow apex facing downward to ensure proper positioning of the embryo. According to Ribatti (2016), maintaining stable incubation temperature and humidity was critical for the viability and uniform growth of the embryo, as fluctuations could lead to developmental defects. To prevent adhesion of the embryo to the shell membrane, eggs were gently rotated twice daily during the first three days of incubation (Kue et al., 2015).

Windowing

On the third day of incubation, a small window (approximately 1–2 cm²) was carefully created at the eggshell's apex to provide future access to the chorioallantoic membrane (CAM). The underlying shell membrane was moistened with sterile saline and gently removed to expose the CAM. The window was then sealed using sterile transparent tape to prevent microbial contamination and dehydration. This technique, described by Nowak-Sliwinska et al. (2014), allowed gas exchange while maintaining embryo viability and facilitated later compound application without disturbing the internal environment of the egg.

Application of Compounds

By the 10th embryonic day, the CAM was well-vascularized, making it ideal for anti-angiogenic testing. The *I. cylindrica* crude extract was applied using a sterile filter paper disk soaked with a measured volume of extract. The disk was gently placed on the CAM surface near visible blood vessels to ensure direct diffusion of the compound. Control embryos received disks soaked in 0.9% saline solution. This method was shown to effectively deliver phytochemicals to the CAM while minimizing physical disturbance of the membrane and was widely used as an alternative to gelatine sponges in CAM assays (Huang et al., 2015; Ribatti, 2016). The eggs were then resealed and returned to the incubator for further development.

Incubation

After treatment application, the egg windows were resealed with sterile transparent tape, and the eggs were returned to the incubator under the same conditions (37.5°C and 60% relative humidity). The eggs remained stationary for an additional 48 to 72 hours to allow the compound to interact with the CAM and potentially modulate angiogenesis. All treatments and observations were conducted before EDD-14 to comply with ethical guidelines, as embryos were not considered capable of experiencing pain before this stage.

Observation and Quantification

After 72 hours post-treatment, the eggs were reopened for observation on EDD-12. The CAM was examined under a high-definition camera, and high-resolution images were captured to document vascular changes. Quantitative analysis of vascular junctions, end-point voxels and maximum branch length was performed using ImageJ software, allowing objective evaluation of the extract's effect on angiogenesis. A reduction in vessel

density or branching was interpreted as evidence of anti-angiogenic activity. This timeline aligns with established CAM protocols and ensures reliable assessment of compound effects on blood vessel formation (Nowak-Sliwinska et al., 2014; Ribatti, 2016).

The study included one control group and three experimental groups. The control group received 0.9% saline, while the experimental groups were treated with 10 µg/mL, 20 µg/mL, and 30 µg/mL concentrations of the plant extract, respectively. The use of 0.9% saline as a negative control is consistent with previous studies, which employed saline solutions to maintain isotonic conditions without introducing biological effects (Vincek et al., 2003). Similar concentration ranges of plant extracts have been used in earlier research to determine dose-dependent biological activity.

Table 2. Experimental Groups

Control Group	Experimental Group (Low Dosage)	Experimental Group (Medium Dosage)	Experimental Group (High Dosage)
0.9% NaCl	<i>Imperata cylindrica crude extract</i>		
10µL per egg	10µg/mL	20µg/mL	30µg/mL

Phase III – Network Pharmacology

Network pharmacology was a modern approach that integrated systems biology, bioinformatics, and pharmacology to explore the complex interactions between bioactive compounds, molecular targets, and biological pathways (Hopkins, 2008). Unlike the traditional “one drug–one target” model, this method emphasized the multi-target mechanisms of natural products, which provided a holistic view of how these compounds exerted therapeutic effects (Li et al., 2014). It became an essential tool for studying medicinal plants such as *I. cylindrica*, which contained diverse phytochemicals that act synergistically to regulate biological processes like angiogenesis. By integrating compound–target prediction, protein–protein interaction networks, and pathway enrichment analysis, network pharmacology enabled the identification of key proteins and signaling pathways influenced by these bioactive compounds (Barabási & Oltvai, 2004). Overall, it provided a systematic framework for connecting natural compounds to their molecular mechanisms, supporting the scientific validation of traditional herbal medicines (Li et al., 2014).

Identification of Active Compounds

Identifying active compounds was the foundation of network pharmacology. Bioactive phytochemicals were screened for their drug-likeness, oral bioavailability, and pharmacokinetic properties using ADME (Absorption, Distribution, Metabolism, Excretion) filters. Studies such as Li et al. (2014) emphasized that identifying active molecules enabled linking specific natural compounds to target pathways in diseases like cancer and inflammation. The phytochemicals of *I. cylindrica* were retrieved from the study of Young-Kyung Jung & Dongyun Shin (2021) titled *Imperata cylindrica: A Review of Phytochemistry, Pharmacology, and Industrial Applications*. The bioactive compounds from the initial list were further filtered through existing studies. The phytochemicals PUBCHEM ID and the canonical SMILES string for each molecule, were obtained from PubChem. The SMILES string is the primary input for the screening software. The screening software that was used was MolSoft, collecting molecular descriptors such as Molecular Weight, Hydrogen Bond Acceptor (HBA), Hydrogen Bond Donor (HBD), Calculated LogP (CLogP) and Drug Likeness Score. Lipinski's Rule of Five was used to filter phytochemicals through Molecular Weight being less than 500 Daltons, HBA less than 10, CLogP less than 5 and HBD less than 5. The MolSoft Drug Likeness Score is a quantitative prediction where a positive value (above 0.00) indicates the molecule has chemical features statistically similar to those of known drugs, suggesting favorable absorption, distribution, metabolism, and excretion (ADME) properties. The prediction of ADME and Toxicological Profiles was made through the software SwissADME, collecting GI absorption (Gastrointestinal Absorption), Blood-Brain Barrier (BBB) penetration, toxicity and solubility.

Prediction of Key Gene/Protein Targets

According to Hopkins (2008), network pharmacology relied on target prediction to reveal the polypharmacological nature of bioactive compounds. The identified phytochemicals will be used for the further steps. For the Drug-Target mining, the SwissTargetPrediction database is used to predict the biological targets (proteins/genes) of the drug molecules using their SMILES chemical structure strings. The results are filtered based on the Probability Score, the top 100 were selected because they are the most relevant targets. While for the disease target mining, the GeneCard database is used to find all genes related to angiogenesis. The genes are filtered using the GIFT (GeneCard Inferior Functionality) Score, with a score above 50% for higher-knowledge and more functional genes. Lastly for the target mapping, the Venn Diagram Tool (Venny 2.0) is used to compare the list of drug targets and the list of disease targets. The resulting common targets are identified as the most important therapeutic targets for the phytochemical to act upon in that disease.

Protein-Protein Interaction (PPI) Network Analysis

Proteins rarely acted alone; angiogenesis was a multi-protein process involving VEGF signaling, ECM remodelling, and inflammatory mediators. PPI networks revealed hub proteins that played central regulatory roles. As demonstrated by Stelzl et al. (2005), PPI network analysis identified essential nodes for therapeutic intervention. STRING is used to visualize the protein-protein interactions between these targets, where the proteins are nodes and the interactions are edges. The CytoHubba plugin from the software CytoScape, was used in the video as a more sophisticated method to precisely rank the common target genes identified in the previous steps, thereby determining the most important Core Targets in the Protein-Protein Interaction (PPI) network.

Pathway Enrichment Analysis (KEGG)

Pathway enrichment connected the compound-target data to specific angiogenic mechanisms. This identified how the extract modulated signaling cascades that drove new blood vessel formation. Kanehisa et al. (2019) emphasized that KEGG pathway enrichment helped interpret high-throughput molecular data into functional biological meaning. The core of the KEGG Pathway Analysis involves using a highly ranked list of matched drug-disease targets as input to the ShinyGO database to identify the specific biological signaling and metabolic pathways they significantly regulate. This is done because KEGG (Kyoto Encyclopedia of Genes and Genomes) provides a comprehensive map of known cellular pathways, and researchers select the most relevant enriched pathways by evaluating three key metrics: maximizing the Gene Count (more of the input genes are involved), maximizing the Fold Enrichment (indicating a stronger association between the genes and the pathway), and minimizing the FDR/P-value (ensuring statistical significance, typically requiring a value less than 0.05).

Gene Ontology (GO) Functional Annotation

GO annotation helped interpret the biological relevance of targets, e.g., identifying those involved in endothelial cell migration, cytokine binding, or receptor signaling. Ashburner et al. (2000) defined GO as a tool to unify biological information and link gene function to system-level processes. The Gene Ontology (GO) Analysis is performed on the core targets to classify their roles across three categories: Biological Process (BP) (broad activities like signal transduction), Cellular Component (CC) (sub-cellular location like the cell membrane), and Molecular Function (MF) (specific biochemical actions such as kinase activity). This functional classification is achieved using ShinyGO, and the most significant functional terms—are selected by prioritizing results with high Fold Enrichment and statistically significant low FDR (False Discovery Rate) values, similar to the criteria used for KEGG analysis.

Target-Pathway-Disease Merge Network Construction

The construction of the final Drug-Target-Pathway (D-T-P) Network involves preparing two key datasets in Excel, each structured as a two-column table with "Node 1" and "Node 2": one for Pathway-Target Interaction and another for Drug-Target Interaction. Both tables are individually imported into Cytoscape to form separate networks, which are then combined using the Tools > Merge > Network function into a single comprehensive network, and a Circular Layout is applied for clear visualization. Finally, the network's visual elements are

customized (e.g., node shapes/colors), and analysis of the Node Degree (connection count) confirms the most crucial point of intervention.

Phase IV – Molecular Docking

Molecular docking was employed to predict the interaction between phytochemicals from *I. cylindrica*, and VEGFR-2 (vascular endothelial growth factor receptor 2), a key regulator of angiogenesis. VEGFR-2 was widely recognized as a primary signaling receptor involved in endothelial cell proliferation, migration, and new blood vessel formation. Its overexpression was closely associated with tumor-induced angiogenesis, making it a critical target in research (Guo et al., 2010). Therefore, targeting VEGFR-2 provided a relevant and biologically significant approach to evaluating the anti-angiogenic potential of therapeutic compounds. Given that the inhibitors within the crude extract are unknown, the docking strategy necessitates the use of two distinct enzyme conformations: the Active (DFG-in) state (PDB ID 3B8R) for identifying potential Type I (ATP-competitive) inhibitors, and the Inactive (DFG-out) state (PDB ID 4ASD) for capturing selective Type II inhibitors. The utilization of both states ensures a comprehensive screening strategy for compounds that may selectively inhibit this key anti-angiogenic target. (Source: PDB entries 3B8R and 4ASD).

In conducting the molecular docking study, the established anti-angiogenic target, VEGFR2, and the Core Target (Top Protein/Gene) that is relevant in angiogenesis, identified through the network pharmacology model will both be utilized to ensure comprehensive validation and mechanism exploration. VEGFR2 will be used to validate the primary anti-angiogenic hypothesis, employing both the Active (DFG-in) state (PDB ID 3B8R) and the Inactive (DFG-out) state (PDB ID 4ASD) to differentiate between Type I and Type II inhibitor binding. Simultaneously, the compound will be docked to the Core Target derived from the Drug-Target-Pathway Network analysis to computationally validate the model's prediction and provide evidence for a potent multi-target mechanism of action, a key characteristic of crude natural extracts.

The results were interpreted based on binding affinity. Binding affinity refers to the predicted strength of interaction between the ligand and the receptor (VEGFR-2), expressed as free energy values (kcal/mol), where more negative values indicate stronger and more favorable binding, suggesting greater potential for receptor inhibition (Kitchen et al., 2004).

Waste Disposal

All waste from the CAM assay, including eggshells, embryo tissues, and plant extracts, will be disposed of following Environmental Management Bureau (EMB) Region XI guidelines. The researchers will comply with Republic Act 9003 and local Davao City ordinances, with waste forwarded to the Material Recovery Facility in Barangay 28-C for proper disposal.

Statistical Analysis

Frequency distribution will first be used to summarize and visualize the spread of data points.

The mean and standard deviation will then be calculated to describe the central tendency and variability of each parameter, including vascular junctions, end-point voxels and maximum branch length.

RESULTS

This section presents the findings and discussions based on the data gathered. The presentation is organized into 4 sections: 1) Preparation and Characterization of *I. cylindrica* Crude Extract; 2) In Vivo Anti-Angiogenic Activity in the CAM Model; 3) In Silico Prediction of Anti-Angiogenic Targets and Pathways; and 4) Computational Validation: Binding Affinity to VEGFR2 and Core Target.

Preparation and Characterization of *I. cylindrica* Crude Extract

The extraction process commenced with 125 g of air-dried, powdered *I. cylindrica* leaves, which underwent maceration in 1.25 L of 80% ethanol. After filtration, a specific volume of 120 mL of the liquid extract was

subjected to rotary evaporation to remove the solvent, yielding a final mass of 30 mg of the dark, concentrated crude extract residue. This extraction resulted in a low overall yield of 0.024% relative to the initial dry plant material, calculated as: Yield (%) = (0.030g / 125g) 100.

For the *in vivo* testing, a primary stock solution was first prepared by dissolving 10mg of the crude extract in 10mL of distilled water, establishing a concentration of 1mg/mL or 1000µg/mL. This stock solution served as the source material for all subsequent experimental doses.

The three working concentrations were prepared precisely via volumetric dilution using distilled water as the diluent, with each final volume totaling 1000µL. The low dose of 10µg/mL was achieved by diluting 10µL of the 1000µL/mL stock with 990µL of distilled water. Similarly, the medium dose 20µg/mL and high dose 30µg/mL were prepared by diluting 20µL with 980µL distilled water and 30µL with 970µL distilled water of the stock solution, respectively. Critically, these freshly prepared working solutions were immediately applied to sterile filter paper discs following preparation. This procedure ensured consistency in the application method for the concentration range of 10 µg/mL, 20 µg/mL, and 30 µg/mL onto the Chorioallantoic Membrane (CAM).

In Vivo Anti-Angiogenic Activity in the CAM Model

A total of 14 fertilized eggs were initially incubated. Following the windowing and candling procedures, only four eggs were identified as viable and subsequently selected for the experimental treatment groups. The prepared solutions of *I. cylindrica* were administered to each of the test eggs via sterile filter paper discs on its 10th day of incubation period. Initial viability screening resulted in a sample size of four eggs. Two days after the administration of the solutions on EDD 12, collaterals or branch points were photographed using a high-definition camera. Each of the CAMs blood vessel density were counted and tabulated on ImageJ to determine the angiogenic effects of the different concentrations.

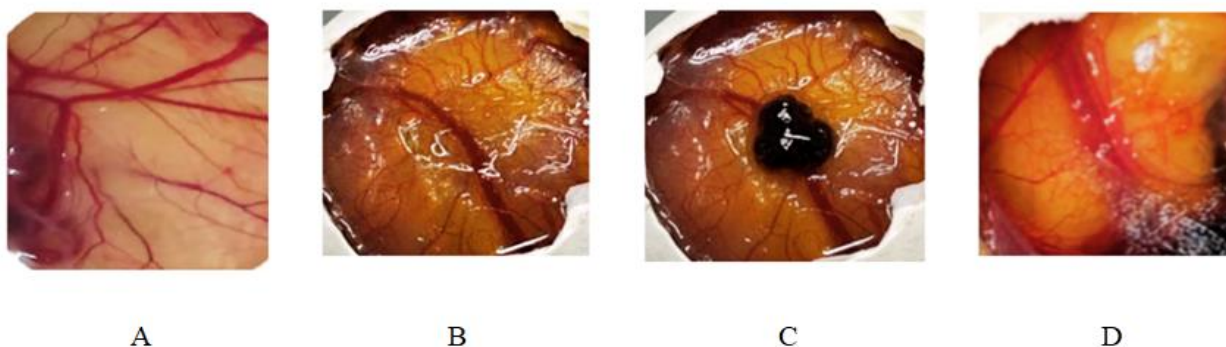


Figure 1. CAM Assay Visualization. (A) Negative Control 0.9% Saline. (B) 10µg/mL *I. cylindrica* Crude extract. (C) 20µg/mL *I. cylindrica* Crude extract. (D) 30µg/mL *I. cylindrica* Crude extract.

The visual comparison between the Negative Control and treated CAM provided compelling qualitative evidence of vascular regression, a rigorous conclusion requires quantitative analysis. To objectively assess the extract's potency, the acquired images were processed using the ImageJ software. This analysis focused on three key anti-angiogenic parameters—Number of Junctions, End-point Voxels, and Maximum Branch Length—to determine the precise magnitude of inhibition across all experimental concentrations.

Mean of Parameters

Table 3. Vascular Junctions

Group	Treatment Concentration	Mean Value	Standard Deviation (Error Bar Length)
1	Negative Control	1.73	±1.90
2	10µg/mL	1.40	±1.40

3	20µg/mL	1.09	±1.12
4	30µg/mL	0.79	±0.78

The data in Table 3 demonstrates that the *I. cylindrica* extract effectively inhibited the formation of vascular junctions in a dose-dependent manner. The Negative Control group established a mean of 1.73 Junctions (representing baseline growth). In sharp contrast, the application of the extract at increasing concentrations resulted in a clear reduction in vascular complexity: The 10µg/ml and 20µg/ml doses reduced the mean count to 1.40 and 1.09 junctions, respectively. The highest dose, 30µg/ml, achieved the greatest biological effect, reducing the mean count to 0.79 junctions.

Table 4. End-Point Voxels

Group	Treatment Concentration	Mean End-Point Voxels	Standard Deviation (±)
1	Negative Control	3.04	1.02
2	10µg/mL	2.57	1.10
3	20µg/mL	1.99	0.99
4	30µg/mL	1.96	0.92

The data in Table 4 demonstrates the effect of the extract on End-point Voxels, which serve as an indicator of initial vessel sprouting and proliferation. The Negative Control group established a mean of 3.04 End-point Voxels (the baseline for initial growth). The application of the extract reduced the count across all doses, with the 30µg/ml and 20µg/ml doses achieving the lowest means of 1.96 and 1.99 End-point Voxels, respectively.

Table 5. Maximum Branch Length

Group	Treatment Concentration	Mean Maximum Branch Length	Standard Deviation (±)
1	Negative Control	4.21	1.09
2	10µg/mL	4.14	1.17
3	20µg/mL	2.11	0.46
4	30µg/mL	2.05	0.92

The data in Table 5 illustrates the extract's effect on Maximum Branch Length, which is a crucial indicator of overall vessel density and structural integrity. The Negative Control group established a baseline mean of 4.21 units of length. The 10µg/ml dose showed minimal change at 4.14, suggesting a threshold concentration is needed for effect. A dramatic drop occurred at the higher concentrations: the 20µg/ml and 30µg/ml doses reduced the mean length to 2.11 and 2.05, respectively.

The quantitative analysis across the primary vascular parameters demonstrated a potent biological anti-angiogenic effect by the *I. cylindrica* extract, supporting the study's hypothesis. The most significant reductions in mean count occurred in Vascular Junctions, dropping from a Negative Control mean of 1.73 to 0.79 at 30µg/ml and Maximum Branch Length, dropping from 4.21 to 2.05 at 30µg/ml, which are both indicators of mature vessel structure. In contrast, End-point Voxels (initial sprouting) showed a lesser reduction, dropping from a mean of 3.04 to 1.96. This differential effect suggests the extract primarily targets the later stages of vascular remodeling and stabilization, rather than initial proliferation. However, it must be noted that this study is fundamentally limited by pseudoreplication due to the biological sample size of N=1 egg per group. Consequently, while the

magnitude of the mean reduction provides strong evidence, the associated high variability (reflected in the large error bars) means that statistical validation is not possible.

Table 6. Comparative Anti-Angiogenic Efficacy (10µg/mL dosage)

Vascular Parameter	Percentage Inhibition (%)
Junctions (Vascular Junctions)	19%
End-Point Voxels	16%
Maximum Branch Length	2%

Presented at Table 6, the chart demonstrating the Comparative Anti-Angiogenic Efficacy at the 10µg/ml Dose confirms that this concentration serves as a threshold dose where the extract begins to exert its inhibitory effects, though at a low magnitude. For Vascular Junctions, the inhibition rate is 19%. For End-point Voxels, the inhibition rate is 16%. For Maximum Branch Length, the inhibition rate is only 2%.

Table 7. Comparative Anti-Angiogenic Efficacy (20µg/mL dosage)

Vascular Parameter	Percentage Inhibition (%)
Junctions (Vascular Junctions)	36%
End-Point Voxels	35%
Maximum Branch Length	50%

Presented in Table 7, the analysis of the 20µg/ml concentration confirms the robust dose-dependent relationship of the extract and provides strong evidence for its primary mechanism. At this concentration, the anti-angiogenic efficacy significantly increases: Maximum Branch Length shows the highest inhibition at 50%; Vascular Junctions show 36% inhibition; and End-point Voxels show 35% inhibition. The sharp increase in inhibition across all parameters compared to the 10µg/ml dose confirms that this concentration effectively crosses the threshold required to engage the inhibitory pathways.

Table 8. Comparative Anti-Angiogenic Efficacy (30µg/mL dosage)

Vascular Parameter	Percentage Inhibition (%)
Junctions (Vascular Junctions)	54%
End-Point Voxels	36%
Maximum Branch Length	51%

Presented in Table 8, the analysis of the 30µg/ml concentration confirms the robust dose-dependent relationship and provides the strongest evidence for the extract's primary mechanism. At this highest tested concentration, the anti-angiogenic efficacy peaks: The highest inhibition is seen in Vascular Junctions 54% and Maximum Branch Length 51%, both representing overall vessel structure and organization. In contrast, End-point Voxels inhibition is significantly lower at 36%.

The experimental data provides strong quantitative and qualitative evidence to support the hypothesis that the *I. cylindrica* extract possesses potent anti-angiogenic properties, acting in a clear dose-dependent manner. The comparative efficacy across the three concentrations 10µg/ml, 20µg/ml, and 30µg/ml confirms that 10µg/ml serves as a low-magnitude threshold, while higher concentrations achieve significant biological inhibition

(Tables 6, 7, and 8). Crucially, the overall trend demonstrates a consistent differential effect: the highest inhibition rates were observed for Vascular Junctions (up to 54%) and Maximum Branch Length (up to 51%), compared to the lower inhibition of End-point Voxels (maximum 36%). This pattern provides compelling evidence that the extract's primary mechanism is targeting the later stages of angiogenesis, specifically disrupting the pathways involved in vessel stabilization and structural remodeling, rather than solely blocking initial endothelial cell proliferation.

In Silico Prediction of Anti-Angiogenic Targets and Pathways

Starting from the 72 phytochemicals of *I. cylindrica*, 27 phytochemicals were identified through existing studies to possess bioactivity, namely, Tricin (Yu et al. 2024), B-sitosterol (Babu & Jayaraman 2020), Jaceidin (Jung & Shin 2021), Caryatin (Jung & Shin 2021), 5,7-Dihydroxy-8-methoxyflavone (Geeng Chen et al. 2008), 5-methoxyflavone (MedChem Express 2025), 5-hydroxyflavone (Montenegro et al. 2017), Flavone (Hostetler et al. 2017), Vanillic acid (Swislocka et al. 2025), Protocatechuic acid (Masella et al. 2012), 4-Hydroxybenzaldehyde (Yao Chen et al. 2021), ferulic acid (Pyrzynska 2024), 2-Methoxyestrone (Morabito et al. 2004), Tabanone (Cerdeira et al. 2012), Phytol (Islam et al. 2020), Daucosterol (Omari et al. 2022), α -Amyrin (Viet et al. 2025), Friedelin (Loll 2023), Caffeic acid (Ray et al. 2024), Salicin (Pal et al. 2024), Ethyl p-hydroxybenzoate (Food S.A. 2025), Palmitic acid (Wang et al. 2023), 5-Hydroxymethylfurfural (Long et al. 2023), N-Acetyl-p-aminophenol (Duan & Zeng 2025), Cylindrin (Li et al. 2023), Isovanillin (PubChem), and p-Vinylguaiacol (Luo et al. 2021).

Presented in Table 9, the 28 phytochemicals were filtered again through Lipinski's Rule of Five, wherein only the compounds that violated one or none of the Ro5 will remain, namely; Tricin, B-sitosterol, Jaceidin, Caryatin, 5,7-Dihydroxy-8-methoxyflavone, 5-methoxyflavone, 5-hydroxyflavone, Flavone, Vanillic acid, Protocatechuic acid, 4-Hydroxybenzaldehyde, ferulic acid, 2-Methoxyestrone, Tabanone, α -Amyrin, Caffeic acid, Salicin, Ethyl p-hydroxybenzoate, 5-Hydroxymethylfurfural, N-Acetyl-p-aminophenol, Isovanillin, and p-Vinylguaiacol remained. Phytol, Friedelin, Palmitic acid and Cylindrins, lipophilicity (MolLogP) was greater than 5 and drug-likeness model score were below 0.00 meaning compounds are too fatty and poorly balanced in its physicochemical properties to be an effective orally administered drug. While, Daucosterol has a molecular weight greater than 500 and lipophilicity (MolLogP) greater than 5 leading to poor overall absorption and 4-Hydroxy-cinnamic acid was identified to be a corrosive, acute toxic and irritant compound in PubChem.

Table 9: Network Pharmacology

Compound	Molecular Formula	Molecular Weight	Number of HBA	Number of HBD	Mol Log P	Drug-Likeness Model
Tricin	C16 H12 O3	252.08	3	0	3.52	0.04
β -sitosterol	C15 H10 O3	238.06	3	1	4.26	0.17
Jaceidin	C15 H10 O2	222.07	2	0	3.86	0.04
Caryatin	C8 H8 O4	168.04	4	2	1.20	-0.18
5,7-Dihydroxy-8-methoxyflavone	C7 H6 O4	154.03	4	3	1.05	0.23
5-Methoxyflavone	C7 H6 O2	122.04	2	1	1.11	-1.49
5-Hydroxyflavone	C10 H10 O4	194.06	4	2	1.61	-0.61
Flavone	C19 H24 O3	300.17	3	1	2.88	0.61
Vanillic acid	C13 H18 O	190.14	1	0	3.58	-0.84

Protocatechuic acid	C20 H40 O	296.31	1	1	7.72 (> 5)	-0.87
4-Hydroxybenzaldehyde	C35 H60 O6	576.44 (>500)	6	4	6.31 (> 5)	0.5
Ferulic acid	C30 H50 O	426.39	1	1	7.77 (> 5)	0.1
2-Methoxyestrone	C30 H50 O	426.39	1	0	7.44 (> 5)	-0.43
Tabanone	C9 H8 O4	180.04	4	3	1.27	-0.35
Phytol	C13 H18 O7	286.11	7	5	-1.17	-1.1
Daucosterol	C9 H10 O3	166.06	3	1	2.24	-0.2
α -Amyrin	C9 H8 O3	164.05	3	2	1.66	-0.81
Friedelin	C16 H32 O2	256.24	2	1	6.64 (> 5)	-0.54
Caffeic acid	C6 H6 O3	126.03	3	1	0.23	-1.64
Salicin	C8 H9 N O2	151.06	2	2	0.79	0
Ethyl p-hydroxybenzoate	C31 H52 O	440.40	1	0	8.57 (> 5)	-0.13
4-Hydroxy-cinnamic acid	C8 H8 O3	152.05	3	1	1.13	-1.54
Palmitic acid	C9 H10 O2	150.07	2	1	2.11	-1.13
5-Hydroxymethylfurfural	C16 H12 O3	252.08	3	0	3.52	0.04
N-Acetyl-p-aminophenol	C15 H10 O3	238.06	3	1	4.26	0.17
Cylindrin	C15 H10 O2	222.07	2	0	3.86	0.04
Isovanillin	C8 H8 O4	168.04	4	2	1.20	-0.18
p-Vinylguaiacol	C7 H6 O4	154.03	4	3	1.05	0.23

Presented in Table 9, the ADME and toxicological profiles were predicted using the SwissADME tool to assess the pharmacological potential of the final candidates. The analysis compares 19 compounds based on key Absorption, Distribution, Metabolism, Excretion, and Toxicity (ADMET) criteria to assess their potential as oral drug candidates. Most compounds adhere well to Lipinski's Rule of Five, suggesting favorable oral bioavailability, and many, such as Protocatechuic Acid and N-Acetyl-p-aminophenol, are predicted to have High GI Absorption and acceptable solubility. However, several compounds face significant liabilities: those like Caryatin, Jaceidin, and 5-methoxyflavone present the highest risk, as they are predicted to be potential hERG inhibitors and pose a CYP inhibition risk, indicating high potential for cardiotoxicity and harmful drug-drug interactions, respectively. Many compounds, including beta-Sitosterol and 2-Methoxyestrone, are predicted to have Low GI Absorption or poor solubility, limiting their oral efficacy.

Crucially, the risks associated with hERG inhibition (cardiotoxicity) and CYP inhibition (drug-drug interactions) are considered less critical or irrelevant, as these are typically concerns for chronic, systemic prescription drugs, not necessarily for leads derived from natural products or those used in non-therapeutic contexts. Furthermore, a critical consideration for botanical products is the principle of synergistic action. The isolated molecule predictions, such as those flagging Low Absorption, do not account for the influence of the complex plant matrix. Other constituents within the extract may function as natural excipients or permeation enhancers, effectively

improving the bioavailability of poorly performing compounds. Similarly, predicted toxicities were considered subject to potential mitigation by co-occurring protective molecules within the extract.

Table 10: ADME and Toxicological Profiles

Compound	Lipinski Rule	GI Absorption	PBB Permeability	Solubility	Toxicity
β -Sitosterol	Violates 1 rule	Low	No	Soluble to moderately soluble	No hERG inhibition, No CYP inhibition
α -Amyrin	Violates 1 rule	Low	Yes	Poorly soluble	No hERG inhibition, No CYP inhibition
2-Methoxyestrone	Yes	Low	No	Poorly soluble	No hERG inhibition, No CYP inhibition
Tricin	Violates 1 rule	Low	No	Soluble to moderately soluble	Potential hERG inhibitor, CYP Inhibitor risk for all isozyms (Yes)
Caryatin	Yes	High	No	Poorly soluble	Potential hERG inhibitor, CYP Inhibitor risk for all isozyms (Yes)
Jaceidin	Yes	High	Yes	Poorly soluble	Potential hERG inhibitor, CYP Inhibitor risk for all isozyms (Yes)
5-methoxyflavone	Yes	High	Yes	Moderately soluble	Potential hERG inhibitor, CYP Inhibitor risk for all isozyms (Yes)
5-hydroxyflavone	Yes	High	Yes	Moderately soluble	Potential hERG inhibitor, CYP Inhibitor risk for all isozyms (Yes)
Flavone	Yes	High	Yes	Soluble to moderately soluble	Potential hERG inhibitor, CYP Inhibitor risk for all isozyms (Yes)
5,7-Dihydroxy-8-methoxyflavone	Yes	High	Yes	Soluble to moderately soluble	Potential hERG inhibitor, CYP Inhibitor risk for all isozyms (Yes)
Salicin	Violates 1 rule	Low	No	Moderately soluble	No hERG inhibition, No CYP inhibition
4Hydroxy--cinnamic acid	Yes	High	No	Soluble to moderately soluble	No hERG inhibition, No CYP inhibition

Ethyl p-hydroxybenzoate	Yes	High	No	Soluble to moderately soluble	No hERG inhibition, No CYP inhibition
4-Hydroxybenzaldehyde	Violates 1 rule	High	No	Soluble to moderately soluble	No hERG inhibition, No CYP inhibition
Vanillic Acid	Violates 1 rule	High	Yes	Poorly soluble	No hERG inhibition, No CYP inhibition
Protocatechuic Acid	Yes	High	Yes	Moderately soluble	No hERG inhibition, No CYP inhibition
Ferulic Acid	Violates 1 rule	High	Yes	Soluble to moderately soluble	No hERG inhibition, No CYP inhibition
Caffeic Acid	Violates 1 rule	High	Yes	Soluble to moderately soluble	No hERG inhibition, No CYP inhibition
N-Acetyl-p-aminophenol	Yes	High	No	Very soluble	No hERG inhibition, No CYP inhibition
Isovanillin	Violates 1 rule	High	Yes	Very soluble	No hERG inhibition, No CYP inhibition
p-Vinylguaiacol	Violates 1 rules	High	No	Soluble to moderately soluble	No hERG inhibition, No CYP inhibition
5-Hydroxymethylfurfural	Violates 1 rules	High	No	Very soluble	No hERG inhibition, No CYP inhibition
Tabanone	Violates 1 rules	High	Yes	Soluble to moderately soluble	No hERG inhibition, No CYP inhibition

The potential pharmacological targets for the identified phytochemicals were predicted using the SwissTargetPrediction database, based on their SMILES chemical structure strings. For each phytochemical, the prediction yielded a diverse set of putative protein/gene targets. To ensure high relevance, the results were filtered, and the top 100 targets for each compound, based on the highest Probability Score, were selected for further analysis. A total of 598 drug-targets were obtained. The set of key genes associated with the disease pathway of angiogenesis was retrieved from the GeneCard database. These genes were subsequently filtered using the GeneCard Inferior Functionality (GIFT) Score to prioritize higher-knowledge and functionally established genes. Only genes with a GIFT Score above 50% were retained, resulting in a final list of 2548 genes considered to be the most relevant disease targets for angiogenesis

Presented in Figure 2, target mapping was performed by comparing the list of 598 drug targets (from SwissTargetPrediction) and the list of 2548 disease targets (from GeneCard) using the Venn Diagram Tool (Venny 2.0). The overlapping region of the Venn diagram identified the common targets, which represent the predicted therapeutic proteins where the phytochemicals are most likely to exert its effect against angiogenesis. While the npn-overlapping section number is the count of items that are unique to that single set. These are the targets only predicted for the drug, but not related to the disease, or vice versa. This comparison yielded 382 common therapeutic targets, including key genes such as VEGFR, COX2 and AKT1. These common targets are hypothesized to be the most important therapeutic targets for the phytochemicals to act upon in this disease.

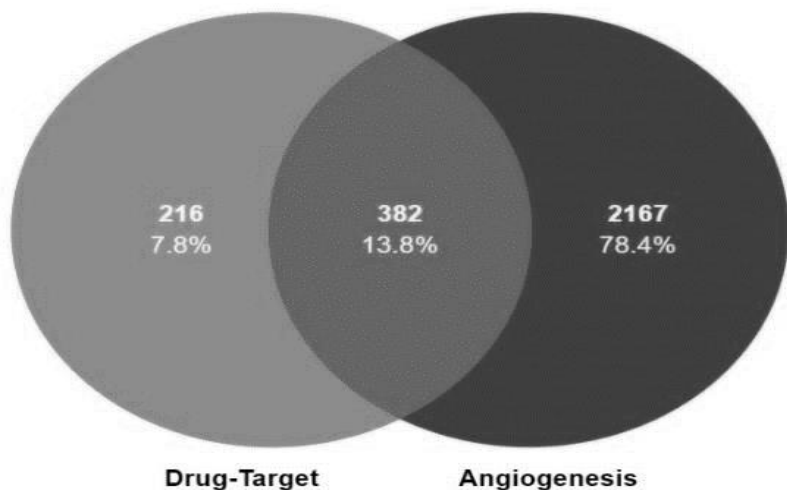


Figure 2. Venny 2.0 results

Presented in Figure 3, a Protein-Protein Interaction (PPI) network was constructed. This analysis aimed to reveal the central regulatory architecture of the identified therapeutic targets. The PPI network was visualized using the STRING database, where the proteins were represented as nodes and their interactions as edges. This visualization confirmed the highly interconnected nature of the targets, suggesting that they belong to common biological pathways essential for the angiogenic process.

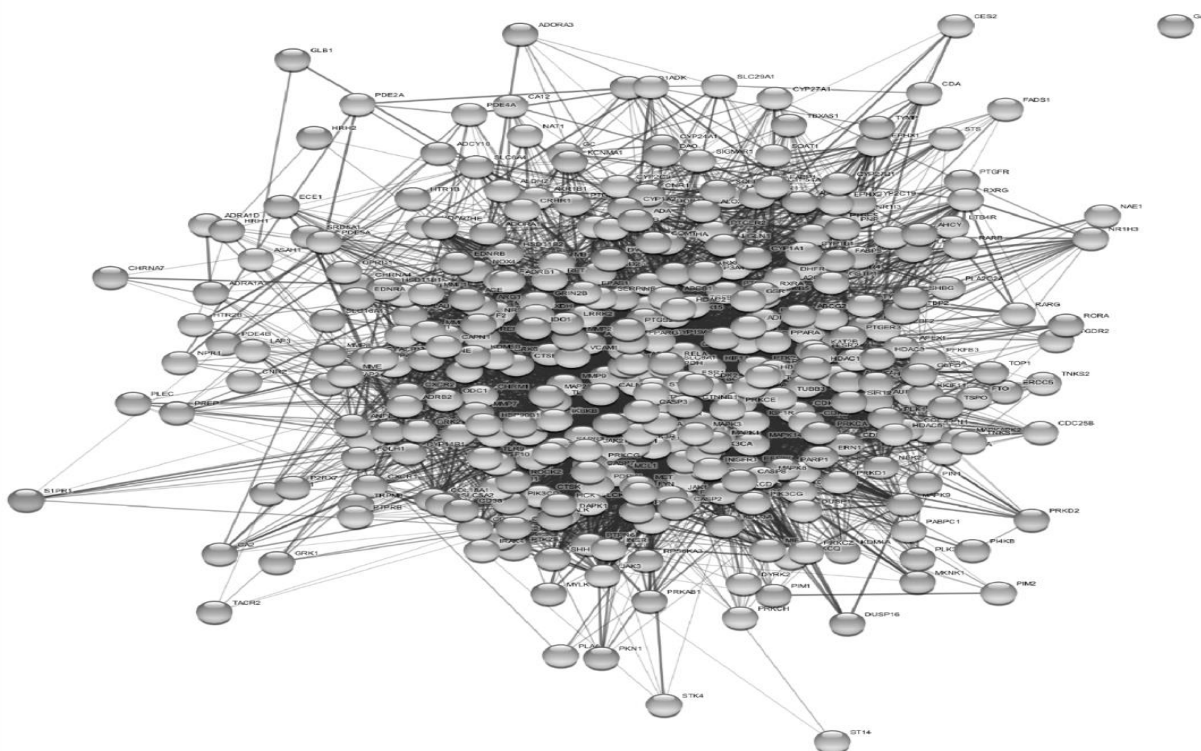


Figure 3. Protein-Protein Interaction (PPI) Network

Presented in Figure 4, following network visualization, a more sophisticated method was employed to rank the importance of the common therapeutic targets precisely. The CytoHubba plugin within the CytoScape software was utilized for this purpose. This tool applied various topological algorithms (e.g., Degree, Betweenness Centrality, Closeness Centrality) to assess the regulatory centrality of each protein within the network. The resulting rankings determined the Core Targets—the hub proteins playing central regulatory roles—which represent the most important therapeutic intervention nodes, as supported by the principles of network analysis. The top 10 proteins identified by the Degree centrality score were designated as the most promising core targets for the phytochemicals. The genes GAPDH, AKT1, TNF, EGFR, SRC, ALB, STAT3, CTNNB3, CASP3 and HSP90AA1 as the top 1, respectively.

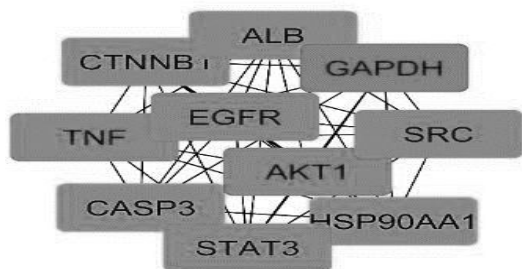


Figure 4. Core Targets by Degree

Presented in Figure 5, the functional relevance of the identified core targets was assessed through KEGG Pathway Enrichment analysis using the ShinyGO database, aiming to elucidate how the phytochemicals might modulate signaling cascades relevant to angiogenesis (Kanehisa et al., 2019). The analysis generated the provided bar plot showing several significantly enriched pathways, which were evaluated based on Fold Enrichment (strength of association), Gene Count (dot size), and Statistical Significance (FDR value, represented by color).

The strong enrichment across multiple disease categories suggests a multifaceted therapeutic potential that addresses upstream drivers of angiogenesis. The pathways exhibiting the highest Fold Enrichment, such as EGFR tyrosine kinase inhibitor resistance, also displayed the strongest statistical significance (dark purple color), indicating robust associations between the input targets and these cellular networks. Pathways central to cell proliferation and survival, such as the HIF-1 signaling pathway and the PI3K-Akt signaling pathway, were highly ranked, confirming that the targets regulate fundamental cellular processes crucial for new blood vessel formation. Furthermore, the prominence of pathways related to metabolic diseases (e.g., Insulin resistance, Lipid and atherosclerosis) and inflammation highlights a potential mechanism where the compounds interfere with the metabolic and inflammatory cues that often trigger pathological angiogenesis.

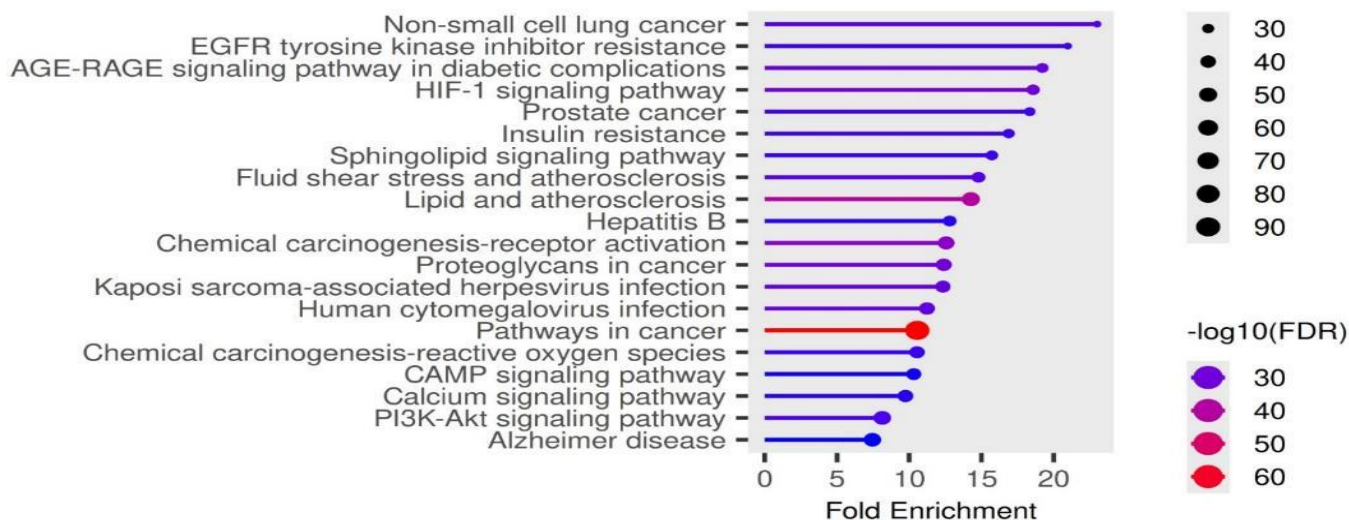


Figure 5. KEGG (Kyoto Encyclopedia of Genes and Genomes)

Presented in Figure 6, the results of a Gene Ontology (GO) Biological Process (BP) enrichment analysis, which identifies the biological functions that are statistically over-represented (enriched) within a given set of genes. The analysis highlights the most significantly affected biological mechanisms related to cellular stress and adaptation. Specifically, the top two enriched terms, "Cellular response to oxygen-containing compound" and "Response to oxygen-containing compound," demonstrate both the highest Fold Enrichment and the highest statistical significance, indicating a minimal chance of false discovery. These processes are also governed by the largest number of differentially expressed genes (indicated by the largest dot size), firmly establishing them as the primary biological pathways perturbed by your experimental condition.

Beyond the oxygen-related responses, other significantly enriched processes include the "Cellular response to chemical stimulus" and "Cell death," suggesting the genes are actively involved in sensing external chemical changes and regulating cell fate. The Fold Enrichment on the x-axis quantifies the magnitude of the enrichment, showing that the oxygen-response terms are enriched by approximately 6-fold compared to chance. The color of the data points represents the statistical confidence, with hotter colors denoting the most robustly significant findings. The overall data points toward a profound and statistically significant impact on the cell's ability to handle oxidative stress, sense chemical changes, and control survival pathways.

The results from the Gene Ontology (GO) Biological Process enrichment analysis are highly relevant to angiogenesis because the most affected pathways—cellular response to oxygen-containing compound and response to stress—represent the core biological triggers of new blood vessel formation. Angiogenesis is primarily initiated by hypoxia (low oxygen), which activates genes for vascular growth; thus, the compounds' strong influence on oxygen-responsive pathways confirms their modulation of this key regulatory trigger. Furthermore, the enrichment of "Cellular response to chemical stimulus" validates that the botanical compounds are biologically active in stress-sensing pathways that lead to cellular adaptation. Finally, the involvement of "Cell death" suggests the compounds are impacting the complex balance of cell proliferation and programmed removal necessary for vascular remodeling and stabilization. Collectively, the GO data provides strong mechanistic evidence that the compounds are acting on the fundamental biological processes that govern the initiation and progression of angiogenesis.

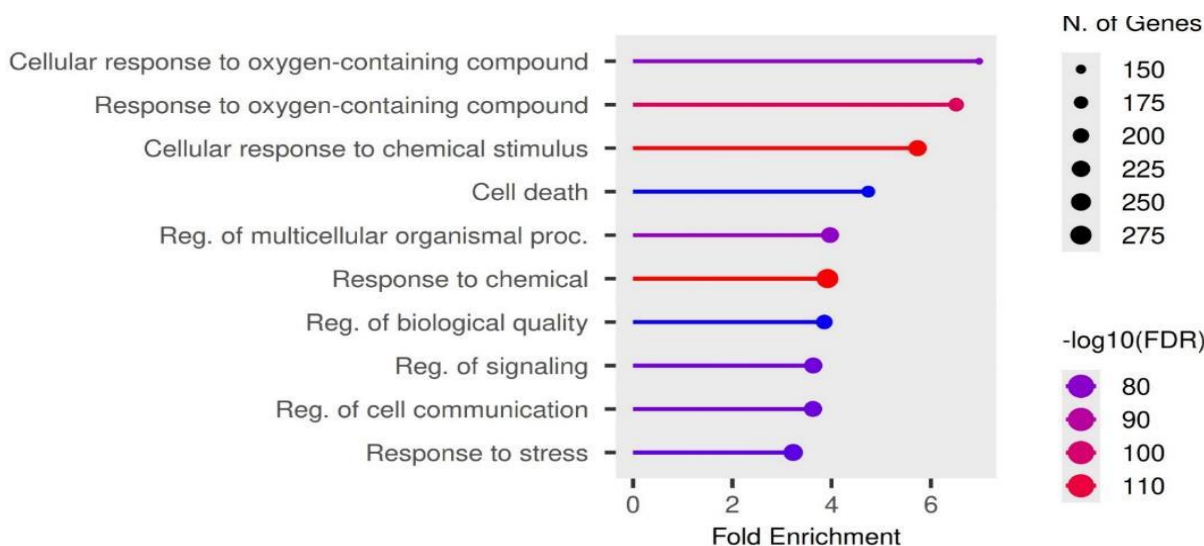


Figure 6. Gene Ontology (GO) Biological Process

Presented in Figure 7, the results of a Gene Ontology (GO) Cellular Component (CC) enrichment analysis, which identifies the subcellular locations that are statistically over-represented in the gene set. The analysis indicates a significant concentration of affected genes within structures critical for cell surface organization and specialization. The most highly enriched terms, including "Membrane raft," "Membrane microdomain," and "Receptor complex," are all components of the plasma membrane involved in organizing and compartmentalizing signaling molecules, mediating cellular interactions, and facilitating signal transduction. Furthermore, the enrichment of terms like "Dendrite," "Synapse," and "Cell junction" suggests a broad influence on specialized structural domains that dictate cell-to-cell communication and architectural organization.

Collectively, the data suggests that the primary biological mechanism involves modulating the functional and structural integrity of the cell periphery and its specialized signaling platforms.

The significant enrichment of membrane-associated and junctional GO Cellular Component terms possesses direct relevance to the process of angiogenesis. The terms "Membrane raft" and "Receptor complex" are fundamentally important because the migration and proliferation of endothelial cells are initiated by the clustering and activation of angiogenic receptors (such as VEGFRs and integrins) within these specialized membrane microdomains. This spatial organization is essential for efficient downstream signaling. Moreover, the enrichment of the "Cell junction" term is highly pertinent, as the regulated disassembly and reassembly of adherens and tight junctions between endothelial cells are prerequisite events for them to sprout, migrate, and establish new vascular lumens. Consequently, the data suggests that the compounds influence angiogenesis by modulating the structural scaffolding, signaling compartmentalization, and junctional integrity of the endothelial cell surface, thereby affecting their ability to sense, move, and form new tubular structures.

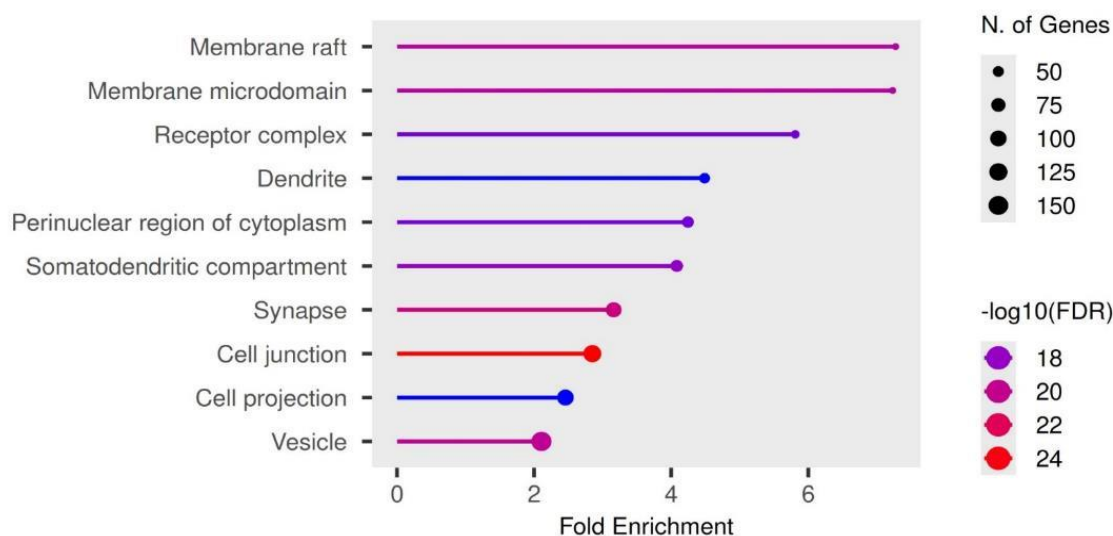


Figure 7. Gene Ontology (GO) Cellular Component.

Presented in Figure 8, the results of a Gene Ontology (GO) Molecular Function (MF) enrichment analysis, which identifies the specific biochemical activities performed by the proteins encoded by your gene set. The analysis clearly indicates that the affected genes are overwhelmingly involved in phosphorylation and enzyme regulation. The terms with the highest Fold Enrichment, statistical significance, and number of genes are "Protein kinase activity," "Protein serine/threonine kinase activity," and "Phosphotransferase activity." Kinases are a class of enzymes that add phosphate groups (a process called phosphorylation) to proteins, acting as the master "on/off" switches for cellular signaling pathways. The high enrichment of "Kinase activity" and "Transferase activity transferring phosphorus-containing groups" confirms that the compounds' primary action is to modulate this fundamental cellular communication mechanism. Secondary terms, such as "Adenyl nucleotide binding" and "Enzyme binding," further support a role in regulating the energy state and functional interactions of enzymatic processes.

The strong enrichment of kinase activity is exceptionally relevant to angiogenesis, as this process is almost entirely controlled by a complex cascade of phosphorylation events. Angiogenesis is triggered by growth factors (like VEGF) binding to receptors on the endothelial cell surface, and these receptors are, in fact, receptor tyrosine kinases. The activation initiates a signal by adding phosphate groups to target proteins. By modulating "Protein kinase activity," compounds are directly interfering with or amplifying the central signal transmission system that controls endothelial cell proliferation, migration, and differentiation into new vessel structures. This finding provides the final piece of the mechanistic puzzle: the compounds target membrane receptors (CC) to influence kinase activity (MF), which ultimately regulates the stress and oxygen responses (BP) necessary for vascular remodeling.

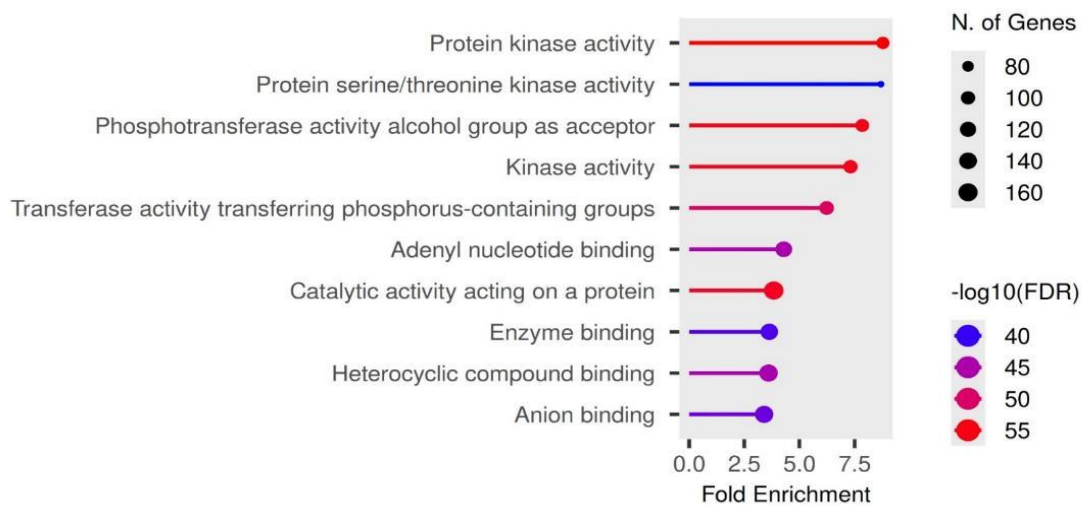


Figure 8. Gene Ontology (GO) Molecular Function

Presented in Figure 9, the final Drug-Pathway-Target (DPT) network was constructed to visualize the complex interplay between the identified botanical compounds, their protein targets, and relevant biological pathways. The network was generated within Cytoscape by merging two distinct interaction datasets: the Pathway-Target Interaction table and the Drug-Target Interaction table, each prepared as a two-column network file (Node 1, Node 2). Following the merger of these two bipartite networks, a Circular Layout was applied for clear visualization of the network components. Visual customization was performed to distinguish node types: compounds were represented by orange triangles, targets by blue circles, and pathways by yellow rectangles. Subsequent analysis focused on Node Degree, which quantifies the number of connections each node possesses. This analysis successfully identified the most highly interconnected targets and pathways (hubs) within the network, thereby confirming the most crucial points of pharmacological intervention for the botanical compounds.

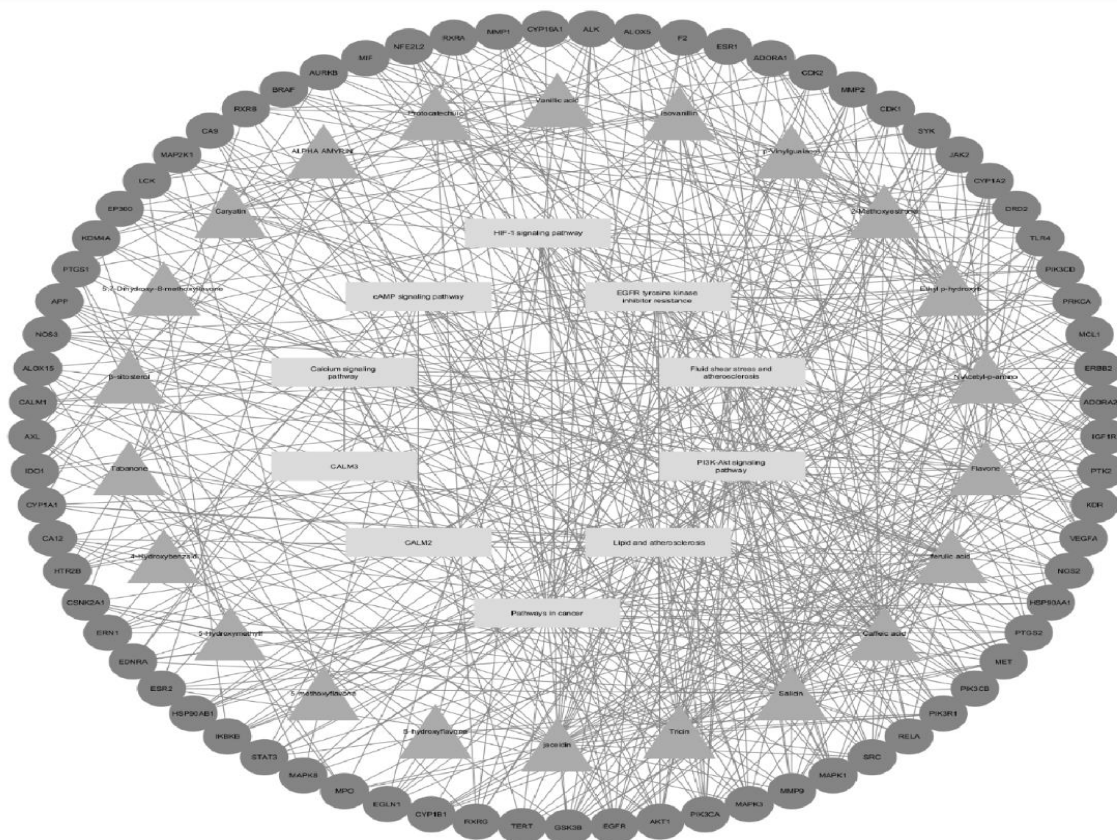


Figure 9. Drug-Pathway-Target Network

Targets with fewer than five interactions were excluded to maximize visualization, and only pathways connected to angiogenesis were included. The effective compounds were ranked in descending order of degree value, with the top 10 predicted to be the key compounds: Salicin, Jaceidin, Caffeic acid, Tricin, Ferulic acid, Ethyl p-hydroxybenzoate, Flavone, N-Acetyl-p-aminophenol, p-Vinylguaiacol, and 2-Methoxyestrone.

Table 11. Top 10 Bioactive Compounds Run Through Network Pharmacology

Rank	Percentage Inhibition (%)	Degree
1	Salicin	34
2	Jaceidin	34
3	Caffeic Acid	33
4	Tricin	27
5	Ferulic Acid	26
6	Ethyl p-hydroxybenzoate	24
7	Flavone	23
8	N-Acetyl-p-aminophenol	23
9	p-Vinylguaiacol	18
10	2-Methoxysterone	17

From the KEGG analysis, pathways that relate to angiogenesis were included in the drug-pathway-target network and those not connected were excluded.

Table 12: Pathways Related to Angiogenesis, Degree in DPT

Name	Type	Degree
EGFR tyrosine kinase inhibitor resistance	Pathway	21
HIF-1 signaling pathway	Pathway	20
Fluid shear stress and atherosclerosis	Pathway	21
CALM2	Pathway	5
CALM3	Pathway	5
Lipid and atherosclerosis	Pathway	31
Pathways in cancer	Pathway	45
cAMP signaling pathway	Pathway	19
Calcium signaling pathway	Pathway	14
PI3K-Akt signaling pathway	Pathway	28

Computational Validation: Binding Affinity to VEGFR2 and Core Target.

Table 13. Molecular Docking Binding Affinity Results

Compound	Active	Inactive	AKT1
Salicin	-7.6	-6.5	-7.2
Jaceidin	-7.2	-6.7	-8.8
Caffeic Acid	-6	-5.7	-6.1
Tricin	-6.9	-5.3	-7.4
Ferulic Acid	-7.1	-5.8	-6.4
Ethyl p-Hydroxybenzoate	-6.8	-5	-5.8
Flavone	-8.3	-6.9	-7.6
N-Acetyl-P-Aminophenol	-5.8	-5	-5.6
P-Vinylguaiacol	-5.7	-5.1	-5.2
2-Methoxyestrone	-8.4	7.3	-8.5

The molecular docking analysis was designed to evaluate the predicted binding strength of *I. cylindrica* phytochemicals against the VEGFR in its ACTIVE and INACTIVE conformations, along with the independent kinase target AKT1. The binding affinity scores, recorded in kcal/mol, reflect the theoretical stability of these molecular interactions, where higher negative values signify superior binding stability. The results reveal several compounds with high affinity for the functional VEGFR ACTIVE state. 2-Methoxyestrone -8.4 kcal/mol and Flavone -8.3 kcal/mol demonstrated the strongest calculated affinities for the functional conformation. Conversely, Jaceidin -8.8 kcal/mol and Caryatin -8.7 kcal/mol were identified as the most potent theoretical binders to the distinct AKT1 kinase target. The overall range of high negative affinities suggests that the crude extract is rich in constituents capable of forming significant inhibitory interactions with both VEGFR and AKT1, both being essential drivers of angiogenesis.

Analysis of conformational selectivity between the VEGFR ACTIVE and VEGFR INACTIVE states provides crucial insight into the putative mechanism of action. The majority of the compounds, including 2-Methoxyestrone, Flavone, Jaceidin, Protocatechuic Acid, Isovanillin, Vanillic Acid, Tricin, Ferulic Acid, Ethyl P-Hydroxybenzoate, N-Acetyl-P-Aminophenol, P-Vinylguaiacol, Tabanone, 5,7-Dihydroxy-8-Methoxyflavone, 4-Hydroxybenzaldehyde, beta-Sitosterol, and 5-Hydroxyflavone, display a measurable preference for binding to the functional VEGFR ACTIVE conformation. This implies a potential mode of action as competitive inhibitors that block the ligand-binding site or compounds that stabilize the active dimeric state of the receptor. In contrast, ALPHA AMYRIN is a unique candidate, exhibiting a slightly higher affinity for the VEGFR INACTIVE conformation -9.0 kcal/mol vs. -8.7 kcal/mol for ACTIVE. This observation suggests a mechanism involving allosteric inhibition by stabilizing the receptor in its non-functional state, effectively preventing VEGFR signaling.

DISCUSSION

The in vivo CAM assay results demonstrated that *I. cylindrica* extract significantly inhibited angiogenesis in a clear dose-dependent pattern. ImageJ analysis revealed that as the concentration of the extract increased, there was a marked reduction in vascular junctions, end-point voxels, and maximum branch length, which are all measures of vascular density and growth. The 10 µg/mL concentration served as the threshold dose, producing

only minor inhibition (19% for junctions, 16% for voxels, and 2% for branch length). At 20 $\mu\text{g/mL}$, inhibition rates increased sharply to approximately 36–50%, and at 30 $\mu\text{g/mL}$, the extract showed its strongest anti-angiogenic activity—54% inhibition of vascular junctions and 51% inhibition of branch length—indicating suppression of vessel complexity and maturity. The data suggest that *I. cylindrica* mainly acts on the later stages of angiogenesis, targeting vessel stabilization rather than initial sprouting. However, due to the limited biological sample size (one egg per treatment), the study is restricted by pseudoreplication, preventing statistical validation. Despite this limitation, the consistency of the dose-response trend provides compelling evidence for the extract's inhibitory potential.

The in-silico network pharmacology analysis supported these biological findings by revealing the molecular mechanisms underlying the observed anti-angiogenic activity. From 72 identified phytochemicals, 27 were recognized as bioactive; KEGG pathway enrichment confirmed that many of their targets were involved in key angiogenic pathways such as the PI3K-Akt, HIF-1, and EGFR signaling cascades, all of which regulate endothelial cell proliferation, migration, and survival (Wang et al., 2020). The Gene Ontology (GO) Biological Process (BP) analysis indicated that the most enriched terms were “cellular response to oxygen-containing compound” and “response to chemical stimulus,” reflecting the compounds' influence on oxidative stress and metabolic signaling—known triggers of new vessel formation (Liu et al., 2023). The Cellular Component (CC) analysis highlighted enrichment in “membrane raft,” “receptor complex,” and “cell junction,” suggesting that the phytochemicals act on membrane-level signaling areas vital for endothelial communication. Meanwhile, the Molecular Function (MF) analysis identified “protein kinase activity” and “phosphotransferase activity” as the top terms, linking the compounds to interference in phosphorylation processes that regulate angiogenic signal transduction (Shiojima & Walsh, 2002). These findings are consistent with established angiogenic mechanisms where VEGFR2 activation drives downstream PI3K/AKT signaling, promoting endothelial cell survival and vascular growth (Berenjabad et al., 2022).

Finally, molecular docking analysis validated these in silico predictions by showing strong binding affinities between the phytochemicals and angiogenesis-related targets. Several compounds, including 2-Methoxyestrone (−8.4 kcal/mol) and Flavone (−8.3 kcal/mol), exhibited the strongest binding to the active form of VEGFR2, while Jaceidin (−8.8 kcal/mol) and Caryatin (−8.7 kcal/mol) showed high affinity for AKT1, a key regulator of vascular growth and survival. These high negative binding energies suggest stable interactions capable of blocking receptor activation or phosphorylation cascades. Interestingly, α -amyrin displayed a preference for binding to the inactive VEGFR2 form (−9.0 kcal/mol), suggesting an allosteric inhibition mechanism. Altogether, the combined results of the CAM assay and computational modeling indicate that *I. cylindrica* suppresses angiogenesis through multi-target mechanisms—interfering with VEGFR2 and AKT1 signaling, modulating kinase activity, and disrupting membrane receptor complexes that regulate endothelial cell behavior.

CONCLUSION

This section presents the conclusions that were drawn out of the findings of the study. This section further offers recommendations as to how the findings of this study can improve practice.

Based on the findings of the study, the following conclusions are drawn by the researchers:

1. The *I. cylindrica* crude extract exhibited a clear dose-dependent anti-angiogenic effect during the CAM assay. Specifically, the highest concentration of 30 $\mu\text{g/mL}$ demonstrated the greatest inhibition.
2. At its peak concentration of 30 $\mu\text{g/mL}$, the extract significantly suppressed vessel development by inhibiting 54% of vascular junctions and 51% of the maximum branch length.
3. In silico analysis identified 27 bioactive compounds targeting key angiogenic pathways such as PI3K-Akt, HIF-1, and EGFR, with Gene Ontology results highlighting effects on oxidative stress response, receptor complexes, and protein kinase activity involved in angiogenesis regulation.

4. Molecular docking confirmed strong binding affinities between compounds (e.g., Jaceidin, Tricin, 2-Methoxyestrone, and Caryatin) and VEGFR2/AKT1, suggesting that *I. cylindrica* acts through multi-target inhibition of angiogenic signaling, supporting its potential as a natural anti-angiogenic agent.
5. The statistical analysis confirms a significant difference in anti-angiogenic activity between the *I. cylindrica* crude extract and the negative control group, as the extract demonstrated a clear ability to inhibit vascular development that was absent from the untreated samples.

ACKNOWLEDGEMENT

We would like to extend our heartfelt gratitude to the EIM student, Mr. Michael L. Estrao, and ICT student, Mr. Gian D. Avelino with Mr. Jessy Arambala, for their invaluable cooperation and technical assistance in the assembly of the study. We are deeply grateful to Mr. Elias M. Casane from the TVL Department for providing the essential tools and equipment, and to Mr. Joelan Puyales and Mr. Michael L. Tumilap, LPT, Master of Biology, and Ph.D., for offering the expert knowledge, funding, and constructive comments that served as a cornerstone for the successful realization of our objectives and provided us with a clearer academic perspective.

Furthermore, we wish to thank our families for being a constant source of inspiration and support throughout this journey, providing the motivation needed to overcome every challenge encountered. Above all, we offer our deepest praise to God, the source of all wisdom and strength, for His guidance and blessings along the way.

REFERENCES

1. A Human Protein-Protein Interaction Network: A Resource for Annotating the Proteome. (2005). *Cell*, 122(6), 957–968. <https://doi.org/10.1016/j.cell.2005.08.029>
2. Abubakar, A., & Haque, M. (2020). Preparation of medicinal plants: Basic extraction and fractionation procedures for experimental purposes. *Journal of Pharmacy and Bioallied Sciences*, 12(1), 1–10. https://doi.org/10.4103/jpbs.jpbs_175_19
3. Al-Ostoot, Fares Hezam, et al. (2021). Tumor Angiogenesis: Current Challenges and Therapeutic Opportunities. *Cancer Treatment and Research Communications*, 28(1), 100422. <https://doi.org/10.1016/j.ctarc.2021.100422>
4. American Cancer Society. (2024). Breast cancer facts & figures. Cancer.org; American Cancer Society. <https://www.cancer.org/research/cancer-facts-statistics/breast-cancer-facts-figures.html>
5. Annese, T., Tamma, R., & Doménico Ribatti. (2022). IKOSA® CAM Assay Application to Quantify Blood Vessels on Chick Chorioallantoic Membrane (CAM). *Methods in Molecular Biology*, 129–139. https://doi.org/10.1007/978-1-0716-2703-7_10
6. Ashburner, M., Ball, C. A., Blake, J. A., Botstein, D., Butler, H., Cherry, J. M., Davis, A. P., Dolinski, K., Dwight, S. S., Eppig, J. T., Harris, M. A., Hill, D. P., Issel-Tarver, L., Kasarskis, A., Lewis, S., Matese, J. C., Richardson, J. E., Ringwald, M., Rubin, G. M., & Sherlock, G. (2000). Gene Ontology: tool for the unification of biology. *Nature Genetics*, 25(1), 25–29. <https://doi.org/10.1038/75556>
7. Azwanida, N. (2015). A Review on the Extraction Methods Use in Medicinal Plants, Principle, Strength and Limitation. *Medicinal & Aromatic Plants*, 04(03). <https://doi.org/10.4172/2167-0412.1000196>
8. Babu, S., & Jayaraman, S. (2020). An update on β -sitosterol: A potential herbal nutraceutical for diabetic management. *Biomedicine & Pharmacotherapy*, 131, 110702. <https://doi.org/10.1016/j.biopha.2020.110702>
9. Barabási, A.-L., & Oltvai, Z. N. (2004). Network biology: understanding the cell's functional organization. *Nature Reviews Genetics*, 5(2), 101–113. <https://doi.org/10.1038/nrg1272>
10. Berenjabad, N. J., Nejati, V., & Rezaie, J. (2022). Angiogenic ability of human endothelial cells was decreased following senescence induction with hydrogen peroxide: possible role of vegfr-2/akt-1 signaling pathway. *BMC Molecular and Cell Biology*, 23(1). <https://doi.org/10.1186/s12860-022-00435-4>
11. Cerdeira, Antonio, Cantrell, Charles, Dayan, Franck, Byrd, John, & Duke, Stephen. (2012). Tabanone, a New Phytotoxic Constituent of Cogongrass (*Imperata cylindrica*). *Weed Science*, 60, 212-218. <https://doi.org/10.2307/41497626>

12. Chen, K. Y., Chen, Y. J., Cheng, C. J., Jhan, K. Y., Chiu, C. H., & Wang, L. C. (2021). 3-Hydroxybenzaldehyde and 4-Hydroxybenzaldehyde enhance survival of mouse astrocytes treated with *Angiostrongylus cantonensis* young adults excretory/secretory products. *Biomedical journal*, 44(6 Suppl 2), S258–S266. <https://doi.org/10.1016/j.bj.2020.11.008>
13. Chen, L. G., Hung, L. Y., Tsai, K. W., Pan, Y. S., Tsai, Y. D., Li, Y. Z., & Liu, Y. W. (2008). Wogonin, a bioactive flavonoid in herbal tea, inhibits inflammatory cyclooxygenase-2 gene expression in human lung epithelial cancer cells. *Molecular nutrition & food research*, 52(11), 1349–1357. <https://doi.org/10.1002/mnfr.200700329>
14. Cleveland Clinic. (2024, February 15). Atherosclerosis: Types, Causes, & Treatments. Cleveland Clinic. <https://my.clevelandclinic.org/health/diseases/16753-atherosclerosis-arterial-disease>
15. Collantes, M. E., Navarro, J., Belen, A., & Gan, R. (2022). Stroke systems of care in the Philippines: Addressing gaps and developing strategies. *Frontiers in Neurology*, 13(1). <https://doi.org/10.3389/fneur.2022.1046351>
16. Costa, J. (2025, October 28). cancer. *Encyclopedia Britannica*. <https://www.britannica.com/science/cancer-disease>
17. Cubillan, L. D., Em-Em Lamento, Lilibeth Manganip, Yau, G. L., Sun, J. K., Aiello, L. P., & Silva, P. S. (2017). Epidemiologic Assessment of Avoidable Blindness and Diabetic Retinopathy in the Philippines. *Investigative Ophthalmology & Visual Science*, 58 (837–837). <https://share.google/sSezE4MFDDpBGenib>
18. Duan, Y., & Zeng, H. (2025). Research Progress on N-Acetyl-4-Aminophenol and Its Toxic Effects. *Modern Health Science*, 8(2), p99. <https://doi.org/10.30560/mhs.v8n2p99>
19. E214 (ethyl p-hydroxybenzoate - what is it? | Properties, application | preservatives | Foodcom S.A. (2025, April 24). Foodcom S.A. <https://foodcom.pl/en/term-e/e214/>
20. Eala, M. A. B., Maslog, E. A. S., Dee, E. C., Ting, F. I. L., Toral, J. A. B., Dofitas, R. B., Co, H. C. S., & Cañal, J. P. A. (2022). Geographic Distribution of Cancer Care Providers in the Philippines. *JCO Global Oncology*, 8. <https://doi.org/10.1200/go.22.00138>
21. El Omari, N., Jaouadi, I., Lahyaoui, M., Benali, T., Taha, D., Bakrim, S., El Menyiy, N., El Kamari, F., Zengin, G., Bangar, S. P., Lorenzo, J. M., Gallo, M., Montesano, D., & Bouyahya, A. (2022). Natural Sources, Pharmacological Properties, and Health Benefits of Daucosterol: Versatility of Actions. *Applied Sciences*, 12(12), 5779. <https://doi.org/10.3390/app12125779>
22. Faihs, L., Firouz, B., Slezak, P., Slezak, C., Weißensteiner, M., Ebner, T., Ghaffari Tabrizi-Wizsy, N., Schicho, K., & Dungal, P. (2022). A Novel Artificial Intelligence-Based Approach for Quantitative Assessment of Angiogenesis in the Ex Ovo CAM-Model. *Cancers*, 14(17), 4273. <https://doi.org/10.3390/cancers14174273>
23. Fallah, A., Sadeghinia, A., Kahroba, H., Samadi, A., Heidari, H. R., Bradaran, B., Zeinali, S., & Molavi, O. (2019). Therapeutic targeting of angiogenesis molecular pathways in angiogenesis-dependent diseases. *Biomedicine & Pharmacotherapy*, 110, 775–785. <https://doi.org/10.1016/j.biopha.2018.12.022>
24. Graf, F., Fahrner, J., Maus, S., Morgenstern, A., Bruchertseifer, F., Venkatachalam, S., Fottner, C., Weber, M., Huelsenbeck, J., Mathias Schreckenberger, Kaina, B., & Matthias Miederer. (2014). DNA Double Strand Breaks as Predictor of Efficacy of the Alpha-Particle Emitter Ac-225 and the Electron Emitter Lu-177 for Somatostatin Receptor Targeted Radiotherapy. 9(2), e88239–e88239. <https://doi.org/10.1371/journal.pone.0088239>
25. Guo, G., Huss, M., Tong, G. Q., Wang, C., Li Sun, L., Clarke, N. D., & Robson, P. (2010). Resolution of cell fate decisions revealed by single-cell gene expression analysis from zygote to blastocyst. *Developmental cell*, 18(4), 675–685. <https://doi.org/10.1016/j.devcel.2010.02.012>
26. Hopkins, A. L. (2008a). Network pharmacology: the next paradigm in drug discovery. *Nature Chemical Biology*, 4(11), 682–690. <https://doi.org/10.1038/nchembio.118>
27. Hostetler, G. L., Ralston, R. A., & Schwartz, S. J. (2017). Flavones: Food Sources, Bioavailability, Metabolism, and Bioactivity. *Advances in nutrition (Bethesda, Md.)*, 8(3), 423–435. <https://doi.org/10.3945/an.116.012948>
28. Jung, Y.-K., & Shin, D. (2021). *Imperata cylindrica*: A Review of Phytochemistry, Pharmacology, and Industrial Applications. *Molecules (Basel, Switzerland)*, 26(5), 1454. <https://doi.org/10.3390/molecules26051454>

29. Kanehisa, M., Furumichi, M., Sato, Y., Ishiguro-Watanabe, M., & Tanabe, M. (2020). KEGG: integrating viruses and cellular organisms. *Nucleic Acids Research*, 49(D1), D545–D551. <https://doi.org/10.1093/nar/gkaa970>
30. Kıyan, H. T., Demirci, B., Başer, K. H. C., & Demirci, F. (2013). The in vivo evaluation of anti-angiogenic effects of Hypericum essential oils using the chorioallantoic membrane assay. *Pharmaceutical Biology*, 52(1), 44–50. <https://doi.org/10.3109/13880209.2013.810647>
31. KUE, C. S., TAN, K. Y., LAM, M. L., & LEE, H. B. (2015). Chick embryo chorioallantoic membrane (CAM): an alternative predictive model in acute toxicological studies for anti-cancer drugs. *Experimental Animals*, 64(2), 129–138. <https://doi.org/10.1538/expanim.14-0059>
32. Kuete, V., Krusche, B., Youns, M., Voukeng, I., Fankam, A. G., Tankeo, S., Lacmata, S., & Efferth, T. (2011). Cytotoxicity of some Cameroonian spices and selected medicinal plant extracts. *Journal of Ethnopharmacology*, 134(3), 803–812. <https://doi.org/10.1016/j.jep.2011.01.035>
33. Lee, J. S., Shukla, S., Kim, J.-A., & Kim, M. (2015). Anti-Angiogenic Effect of Nelumbo nucifera Leaf Extracts in Human Umbilical Vein Endothelial Cells with Antioxidant Potential. *PLOS ONE*, 10(2), e0118552. <https://doi.org/10.1371/journal.pone.0118552>
34. Li, X., Huang, X., Feng, Y., Wang, Y., Guan, J., Deng, B., Chen, Q., Wang, Y., Chen, Y., Wang, J., Yeong, J., & Hao, J. (2023). Cylindrin from Imperata cylindrica inhibits M2 macrophage formation and attenuates renal fibrosis by downregulating the LXR- α /PI3K/AKT pathway. *European Journal of Pharmacology*, 950, 175771–175771. <https://doi.org/10.1016/j.ejphar.2023.175771>
35. Liu, Z.-L., Chen, H.-H., Zheng, L.-L., Sun, L.-P., & Shi, L. (2023). Angiogenic signaling pathways and anti-angiogenic therapy for cancer. *Signal Transduction and Targeted Therapy*, 8(1). <https://doi.org/10.1038/s41392-023-01460-1>
36. Long, Y., Zhu, M., Ma, Y., Huang, Y., Gan, B., Yu, Q., Xie, J., & Chen, Y. (2023). Variation of bioactive compounds and 5-hydroxymethyl furfural in coffee beans during the roasting process using kinetics approach. *Food Chemistry Advances*, 2, 100242–100242. <https://doi.org/10.1016/j.focha.2023.100242>
37. Lugano, R., Ramachandran, M., & Dimberg, A. (2020). Tumor angiogenesis: causes, consequences, challenges and opportunities. *Cellular and Molecular Life Sciences: CMLS*, 77(9), 1745–1770. <https://doi.org/10.1007/s00018-019-03351-7>
38. Luo, Y., Wang, C.-Z., Sawadogo, R., Yuan, J., Zeng, J., Xu, M., Tan, T., & Yuan, C.-S. (2021). 4-Vinylguaicol, an Active Metabolite of Ferulic Acid by Enteric Microbiota and Probiotics, Possesses Significant Activities against Drug-Resistant Human Colorectal Cancer Cells. *ACS Omega*, 6(7), 4551–4561. <https://doi.org/10.1021/acsomega.0c04394>
39. Malabanan-Cabebe, C. G., et al. (2024). Clinical outcomes of retinoblastoma patients in Davao Region. [Article]. *PMC*, PMC11151136. <https://pubmed.ncbi.nlm.nih.gov/articles/PMC11151136/>
40. Masella, R., Santangelo, C., D'Archivio, M., Li Volti, G., Giovannini, C., & Galvano, F. (2012). Protocatechuic acid and human disease prevention: biological activities and molecular mechanisms. *Current medicinal chemistry*, 19(18), 2901–2917. <https://doi.org/10.2174/092986712800672102>
41. Montenegro, C. D. A., Gonçalves, G. F., Oliveira Filho, A. A. d., Lira, A. B., Cassiano, T. T. M., Lima, N. T. R. d., Barbosa-Filho, J. M., Diniz, M. D. F. F. M., & Pessôa, H. L. F. (2017). In Silico Study and Bioprospection of the Antibacterial and Antioxidant Effects of Flavone and Its Hydroxylated Derivatives. *Morabito, A., Sarmiento, R., P. Bonginelli, & Gasparini, G. (2004). Antiangiogenic strategies, compounds, and early clinical results in breast cancer. 49(2), 91–107. https://doi.org/10.1016/s1040-8428(03)00168-9*
42. National Cancer Institute. (2018, April 2). Angiogenesis Inhibitors. National Cancer Institute; Cancer.gov. <https://www.cancer.gov/about-cancer/treatment/types/immunotherapy/angiogenesis-inhibitors-fact-sheet>
43. Nishida, N., Yano, H., Nishida, T., Kamura, T., & Kojiro, M. (2006). Angiogenesis in cancer. *Vascular Health and Risk Management*, 2(3), 213–219. <https://doi.org/10.2147/vhrm.2006.2.3.213>
44. Nowak-Sliwinska, P., Segura, T., & Iruela-Arispe, M. L. (2014). The chicken chorioallantoic membrane model in biology, medicine and bioengineering. *Angiogenesis*, 17(4), 779–804. <https://doi.org/10.1007/s10456-014-9440-7>
45. Pal, R. S., Pal, Y., Lalitha Chaitanya, M. V. N., Mazumder, A., Khurana, N., & Tharu, P. K. (2024). Discerning the Multi-dimensional Role of Salicin: Bioactive Glycoside Beyond Analgesic: Different

- Perspectives. Current Drug Therapy, 19(7), 757–764. <https://doi.org/10.2174/0115748855272391231114042540>
46. Patumbon, R. G. G. (2023, July 25). SPMC-ACC notes increasing cancer patients for 2022. SunStar Davao. <https://www.sunstar.com.ph/davao/local-news/spmc-acc-notes-increasing-cancer-patients-for-2022>
 47. Philippine Statistics Authority. (2022). Special Release: Registered Deaths in Davao Region, 2020. <https://rso11.psa.gov.ph/sites/default/files/Attachment/Special%20Release%20Registered%20Deaths%20in%20Davao%20Region%202020.pdf>
 48. Pyrzynska, K. (2024). Ferulic Acid—A Brief Review of Its Extraction, Bioavailability and Biological Activity. *Separations*, 11(7), 204. <https://doi.org/10.3390/separations11070204>
 49. Ribatti, D. (2017). The chick embryo chorioallantoic membrane (CAM) assay. *Reproductive Toxicology*, 70, 97–101. <https://doi.org/10.1016/j.reprotox.2016.11.004>
 50. Seo, E.-J., Kuete, V., Kadioglu, O., Krusche, B., Schröder, S., Greten, H. J., Arend, J., Lee, I.-S., & Efferth, T. (2013). Antiangiogenic Activity and Pharmacogenomics of Medicinal Plants from Traditional Korean Medicine. *Evidence-Based Complementary and Alternative Medicine*, 2013, 1–13. <https://doi.org/10.1155/2013/131306>
 51. Shiojima, I., & Walsh, K. (2002). Role of Akt Signaling in Vascular Homeostasis and Angiogenesis. *Circulation Research*, 90(12), 1243–1250. <https://doi.org/10.1161/01.res.0000022200.71892.9f>
 52. Shukla, U. V., & Tripathy, K. (2023). Diabetic Retinopathy. PubMed; StatPearls Publishing. <https://www.ncbi.nlm.nih.gov/books/NBK560805/>
 53. Singh, S. K., Shrivastava, S., Mishra, A. K., Kumar, D., Pandey, V. K., Srivastava, P., Pradhan, B., Behera, B. C., Bahuguna, A., & Baek, K. H. (2023). Friedelin: Structure, Biosynthesis, Extraction, and Its Potential Health Impact. *Molecules (Basel, Switzerland)*, 28(23), 7760. <https://doi.org/10.3390/molecules28237760>
 54. Staton, C. A., Reed, M. W. R., & Brown, N. J. (2009). A critical analysis of current in vitro and in vivo angiogenesis assays. *International Journal of Experimental Pathology*, 90(3), 195–221. <https://doi.org/10.1111/j.1365-2613.2008.00633.x>
 55. Swislocka, R., Kowalczyk, N., Dabrowska, A. et al. (2025). Spectroscopic, antioxidant and cytotoxicity studies of vanillic acids. *Scientific Reports*, 15, 31396. <https://doi.org/10.1038/s41598-025-13965-6>
 56. Szekanecz, Z., & Koch, A. E. (2009). Angiogenesis and its targeting in rheumatoid arthritis. *Vascular Pharmacology*, 51(1), 1–7. <https://doi.org/10.1016/j.vph.2009.02.002>
 57. Valiatti, F. B., Crispim, D., Benfica, C., Valiatti, B. B., Kramer, C. K., & Canani, L. H. (2011). Papel do fator de crescimento vascular endotelial na angiogênese e na retinopatia diabética. *Arquivos Brasileiros de Endocrinologia & Metabologia*, 55(2), 106–113. <https://doi.org/10.1590/s0004-27302011000200002>
 58. Viet, T. D., Anh, L. H., Xuan, T. D., & Dong, N. D. (2025). The Pharmaceutical Potential of α - and β -Amyrins. *Nutraceuticals*, 5(3), 21. <https://doi.org/10.3390/nutraceuticals5030021>
 59. Vishwanatha, J., & Castañeda-Gill, J. (2016). Antiangiogenic mechanisms and factors in breast cancer treatment. *Journal of Carcinogenesis*, 15(1), 1. <https://doi.org/10.4103/1477-3163.176223>
 60. Wang, X., Bove, A. M., Simone, G., & Ma, B. (2020). Molecular Bases of VEGFR-2-Mediated Physiological Function and Pathological Role. *Frontiers in Cell and Developmental Biology*, 8(599281). <https://doi.org/10.3389/fcell.2020.599281>
 61. Wang, X., Zhang, C., & Bao, N. (2023). Molecular mechanism of palmitic acid and its derivatives in tumor progression. *Frontiers in Oncology*, 13. <https://doi.org/10.3389/fonc.2023.1224125>
 62. World Health Organization. (2023). Rheumatoid arthritis. World Health Organization. <https://www.who.int/news-room/fact-sheets/detail/rheumatoid-arthritis>
 63. Yan, F., Sun, S., & Wu, H. (2025). The “angiogenesis-plaque stability paradox” in atherosclerosis pathogenesis. *Frontiers in Cardiovascular Medicine*, 12. <https://doi.org/10.3389/fcvm.2025.1659006>
 64. Yoo, S. Y., & Kwon, S. M. (2013). Angiogenesis and Its Therapeutic Opportunities. *Mediators of Inflammation*, 2013, 1–11. <https://doi.org/10.1155/2013/127170>
 65. Yu, R., Zhang, Y., Wang, T., Duan, J., & Li, X. (2024). Effect of Tricin on cardiomyocyte damage caused by diabetic cardiomyopathy (DCM). *BMC Cardiovascular Disorders*, 24(1), 668. <https://doi.org/10.1186/s12872-024-04295-y>

-
66. Zhou, S., Chu, H., Jin, G., Cui, J., & Zhen, X. (2014). Effects of SKF83959 on the excitability of hippocampal CA1 pyramidal neurons: a modeling study. *Acta Pharmacologica Sinica*, 35(6), 738–751. <https://doi.org/10.1038/aps.2014.23b>
67. 5-Methoxyflavone (2025). MedchemExpress.com. <https://www.medchemexpress.com/5-Methoxyflavone.html>